



OPEN

Cytokine release syndrome-like serum responses after COVID-19 vaccination are frequent and clinically inapparent under cancer immunotherapy

Thomas Walle^{1,2,3,19}✉, Sunanjay Bajaj^{1,2,19}, Joscha A. Kraske², Thomas Rösner², Christiane S. Cussigh⁴, Katharina A. Kälber⁴, Lisa Jasmin Müller⁵, Sophia Boyoung Strobel⁴, Jana Burghaus⁴, Stefan M. Kallenberger², Christoph K. Stein-Thöringer^{2,6}, Maximilian Jenzer², Antonia Schubert^{2,3,7,8}, Steffen Kahle², Anja Williams², Birgit Hoyler¹, Lin Zielske⁹, Renate Skatula⁹, Stefanie Sawall¹, Mathias F. Leber^{1,2}, Russell Z. Kunes¹⁰, Johannes Krisam¹¹, Carlo Fremd^{2,12}, Andreas Schneeweiss¹², Jürgen Krauss², Leonidas Apostolidis², Anne Katrin Berger², Georg M. Haag^{2,13}, Stefanie Zschäbitz², Niels Halama^{2,14,15}, Christoph Springfield², Romy Kirsten⁹, Jessica C. Hassel⁴, Dirk Jäger^{2,13}, NCT ANTICIPATE Investigators* and Guy Ungerechts^{1,2,16,17}

Patients with cancer frequently receive immune-checkpoint inhibitors (ICIs), which may modulate immune responses to COVID-19 vaccines. Recently, cytokine release syndrome (CRS) was observed in a patient with cancer who received BTN162b2 vaccination under ICI treatment. Here, we analyzed adverse events and serum cytokines in patients with 23 different tumors undergoing ($n = 64$) or not undergoing ($n = 26$) COVID-19 vaccination under ICI therapy in a prospectively planned German single-center cohort study ($n = 220$). We did not observe clinically relevant CRS (\geq grade 2) after vaccination (95% CI 0–5.6%; Common Terminology of Adverse Events v.5.0) in this small cohort. Within 4 weeks after vaccination, serious adverse events occurred in eight patients (12.5% 95% CI 5.6–23%): six patients were hospitalized due to events common under cancer therapy including immune related adverse events and two patients died due to conditions present before vaccination. Despite absence of CRS symptoms, a set of pairwise-correlated CRS-associated cytokines, including CXCL8 and interleukin-6 was >1.5-fold upregulated in 40% (95% CI 23.9–57.9%) of patients after vaccination. Hence, elevated cytokine levels are common and not sufficient to establish CRS diagnosis.

Patients with solid tumors have an increased fatality risk after infection with the SARS-CoV-2 coronavirus¹. Patients with cancer have therefore been prioritized for vaccination against SARS-CoV-2 (COVID-19 vaccination) in many countries^{2,3}. Approved vaccines in Europe and the United States use messenger RNA lipid nanoparticles or viral vectors to transiently transfect/transduce a SARS-CoV-2 spike mRNA/transgene, which is translated in the patient's healthy cells at the site of vaccination, thus strongly inducing cellular and humoral adaptive immunity^{4–8}. However, patients with cancer were underrepresented in clinical phase III trials leading to US Food and Drug Administration and European Medicines Agency approval of these vaccines^{6,7,9}. Moreover, an increasing number of patients with cancer receive immunomodulatory cancer therapies, mostly ICIs blocking the PD-1–PD-L1

coinhibitory axis for T-cell activation¹⁰. As ICIs lead to reactivation of tumor antigen-reactive T cells, it is possible that ICIs may also influence activation of SARS-CoV-2 spike protein (S1)-specific T cells. This increased T-cell activation may lead to massive cytokine release and subsequent clinical reactions. The body's systemic response to the resulting release of multiple inflammatory cytokines from T and myeloid cells is called CRS. CRS manifests itself in fever, hypotension, hypoxia and multiorgan dysfunction at later stages¹¹. Most frequently such responses are observed after adoptive T-cell therapies, bispecific antibodies to the CD3 co-receptor or severe infection¹². CRS is commonly graded according to the Common Terminology of Adverse Events (CTCAE) or the American Society for Transplantation and Cellular Therapy (ASTCT) consensus grading^{11,12}; however, fever $\geq 38^\circ\text{C}$ alone is sufficient to establish CTCAE

¹Clinical Cooperation Unit Virotherapy, German Cancer Research Center (DKFZ), Heidelberg, Germany. ²Department of Medical Oncology, National Center for Tumor Diseases, Heidelberg University Hospital, Heidelberg, Germany. ³German Cancer Consortium (DKTK), Heidelberg, Germany.

⁴Department of Dermatology, National Center for Tumor Diseases, Heidelberg University Hospital, Heidelberg, Germany. ⁵Department of Hematology, University Hospital Heidelberg, Heidelberg, Germany. ⁶Division Microbiome and Cancer, German Cancer Research Center (DKFZ), Heidelberg, Germany.

⁷BioQuant & Department of Cell and Molecular Biology, Heidelberg University, Heidelberg, Germany. ⁸Division Signaling and Functional Genomics, German Cancer Research Center (DKFZ), Heidelberg, Germany. ⁹NCT Liquid Biobank, National Center for Tumor Diseases (NCT), Heidelberg, Germany.

¹⁰Department of Statistics, Columbia University, New York, NY, USA. ¹¹Institute of Medical Biometry, Heidelberg University, Heidelberg, Germany. ¹²Division of Gynecological Oncology, National Center for Tumor Diseases (NCT), Heidelberg, Germany. ¹³Clinical Cooperation Unit Applied Tumor-Immunity, German Cancer Research Center (DKFZ), Heidelberg, Germany.

¹⁴Department of Translational Immunotherapy, German Cancer Research Center (DKFZ), Heidelberg, Germany. ¹⁵Helmholtz Institute for Translational Oncology (HITRON), Mainz, Germany. ¹⁶CanVirex, Heidelberg, Germany. ¹⁷Ottawa Hospital Research Institute, Cancer Therapeutics Program, Ottawa, Ontario, Canada. ¹⁹These authors contributed equally Thomas Walle, Sunanjay Bajaj. *A list of authors and their affiliations appears at the end of the paper. ✉e-mail: t.walle@dkfz.de

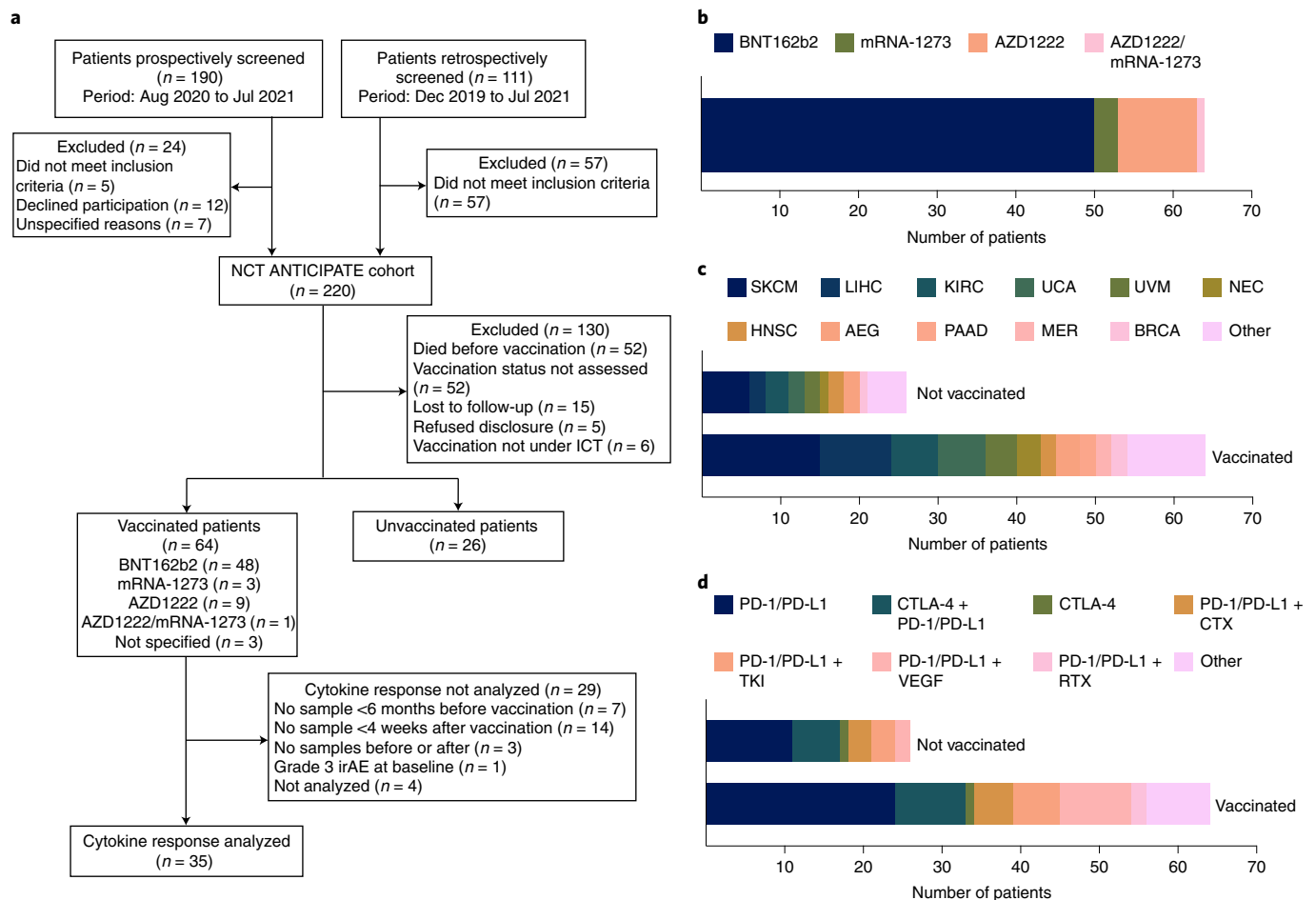


Fig. 1 | A pan-tumor cohort study across diverse immune combination therapies. a, CONSORT flow chart indicating patient screening data and cohorts for subsequent data analysis. **b**, Stacked bar-graph depicting the type of COVID-19 vaccination for vaccinated patients ($n = 64$). **c**, Stacked bar graph indicating tumor types of vaccinated ($n = 64$) and unvaccinated ($n = 26$) patients. AEG, adenocarcinoma of the esophagogastric junction; BRCA, breast cancer; HNSC, head and neck squamous cell carcinoma; KIRC, renal cell carcinoma; LIHC, liver hepatocellular carcinoma; MER, Merkel cell carcinoma; NEC, neuroendocrine carcinoma; PAAD, pancreatic adenocarcinoma; SKCM, skin melanoma; UCA, urothelial carcinoma; UVM, uveal melanoma. **d**, Stacked bar-graph indicating immunotherapies of vaccinated ($n = 64$) and unvaccinated ($n = 26$) patients. CTX, chemotherapy; RTX, radiotherapy; TKI, tyrosine kinase inhibitor.

grade 1 CRS, which does not account for mild fever as part of many appropriate immune reactions¹². Hence, an exhaustive differential diagnosis is essential in establishing CRS¹².

Au et al. recently reported a patient with CRS without evidence for infection after COVID-19 vaccination under ICI therapy¹³. This patient required hospitalization due to fever, thrombocytopenia (grade 3 CTCAE 4.03 and grade 1 ASTCT) as well as increased C-reactive protein (CRP) levels ($\text{CRP} > 200 \text{ mg l}^{-1}$) and CRS-associated cytokine release¹³. This observation prompted questions about the frequency of CRS in patients with cancer under ICI treatment¹³ and whether cytokine profiles could be explored to identify ICI-treated patients with cancer at risk for CRS at early stages.

Here, we assessed adverse events (AEs), clinical laboratory data and serum cytokine responses in patients undergoing combined ICI and COVID-19 vaccination as an exploratory end point of a prospectively registered German single-center cohort study.

Results

A pan-tumor cohort study across immune combination therapies. Between 2 December 2019 and 20 July 2021, we screened 301 patients, of which 190 were screened prospectively and 111 retrospectively as defined in the trial protocol (German Clinical Trials

Register, DRKS00022890). We recruited 220 patients with advanced solid tumors undergoing ICI therapy at our center (Fig. 1a). These patients received regular blood sampling before and during therapy and were monitored for AEs. We assessed the COVID-19 vaccination status of the patients within the cohort during treatment follow-up and identified 64 patients who received a COVID-19 vaccine while under ICI therapy and 26 patients who did not (Fig. 1a,b). The remaining patients either died before the vaccine was widely available ($n = 52$), did not have their vaccination status assessed ($n = 52$), were lost to follow-up ($n = 15$), refused to disclose their vaccination status ($n = 5$) or received COVID-19 vaccinations before ICI therapy ($n = 6$) (Fig. 1a).

We focused further analyses on the 90 patients with known vaccination status (Table 1 and Supplementary Table 1). A total of 23 cancer types were represented within this patient group, the most frequent being skin melanoma ($n = 21$), hepatocellular carcinoma ($n = 11$) and renal cell carcinoma ($n = 9$) (Table 1 and Fig. 1c). Our study included fewer female than male patients, a bias possibly resulting from the recruitment of few gynecological malignancies (Table 1). Therapies included a variety of combinatorial immunomodulatory therapies, most frequently anti-PD-1/PD-L1 monotherapy ($n = 35$), combined anti-PD-1 and anti-CTLA-4 therapy

Table 1 | Characteristics of analyzed patients at baseline

| Characteristic | Vaccinated (n = 64) | Unvaccinated (n = 26) | Total (n = 90) |
|---|---------------------|-----------------------|----------------|
| Patient recruitment characteristics | | | |
| Vaccination period (MM/YY-MM/YY) | 01/21-07/21 | - | 01/21-07/21 |
| Follow-up from first vaccine, days (median) | 24-259 (169) | - | 24-259 (169) |
| Start of ICI period (MM/YY-MM/YY) | 03/20-05/21 | 07/20-07/21 | 03/20-07/21 |
| Follow-up from ICI, days (median) | 44-574 (254) | 30-441 (203.5) | 30-574 (229) |
| Vaccination type, n (%) | | | |
| BNT162b2 | 50 (78.1) | - | 50 (55.6) |
| mRNA-1273 | 3 (4.7) | - | 3 (3.3) |
| AZD1222 | 10 (15.6) | - | 10 (11.1) |
| AZD1222/mRNA-1273 | 1 (1.6) | - | 1 (1.1) |
| Sex, n (%) | | | |
| Male | 44 (68.8) | 19 (73.1) | 63 (70.0) |
| Female | 20 (31.3) | 7 (26.9) | 27 (30.0) |
| Age group at treatment, years n (%) | | | |
| 18-60 | 19 (29.7) | 7 (26.9) | 26 (28.9) |
| >60 | 45 (70.3) | 19 (73.1) | 64 (71.1) |
| Insurance type, n (%) | | | |
| General | 55 (85.8) | 22 (84.6) | 77 (85.6) |
| Private | 9 (14.2) | 4 (15.4) | 13 (14.4) |
| ECOG, n (%) | | | |
| 0 | 11 (17.2) | 7 (26.9) | 18 (20.0) |
| 1 | 46 (71.9) | 13 (50.0) | 59 (65.6) |
| 2 | 7 (10.9) | 4 (15.4) | 11 (12.2) |
| 3 | 0 (0.0) | 2 (7.7) | 2 (2.2) |
| 4-5 | 0 (0.0) | 0 (0.0) | 0 (0.0) |
| Cancer type, n (%) | | | |
| Melanoma | 15 (23.4) | 6 (23.1) | 21 (23.3) |
| Hepatocellular carcinoma | 9 (14.1) | 2 (7.7) | 11 (12.2) |
| Renal clear cell carcinoma | 6 (9.4) | 3 (11.5) | 9 (10.0) |
| Urothelial carcinoma | 6 (9.4) | 2 (7.7) | 8 (8.9) |
| Uveal melanoma | 4 (6.3) | 2 (7.7) | 6 (6.7) |
| Neuroendocrine carcinoma | 3 (4.7) | 1 (3.8) | 4 (4.4) |
| H&N squamous carcinoma | 2 (3.1) | 2 (7.7) | 4 (4.4) |
| Adenocarcinoma of the EG junction | 3 (4.7) | 2 (7.7) | 5 (5.6) |
| Pancreatic adenocarcinoma | 2 (3.1) | - | 2 (2.2) |
| Merkel cell carcinoma | 2 (3.1) | - | 2 (2.2) |
| Breast cancer | 2 (3.1) | 1 (3.8) | 3 (3.3) |
| Other ^a | 10 (15.6) | 5 (19.2) | 15 (16.7) |
| UICC stage at diagnosis, n (%) | | | |
| I | 8 (12.5) | 4 (15.4) | 12 (13.3) |

Continued

Table 1 | Characteristics of analyzed patients at baseline (continued)

| Characteristic | Vaccinated (n = 64) | Unvaccinated (n = 26) | Total (n = 90) |
|---|---------------------|-----------------------|----------------|
| II | 10 (15.6) | 6 (23.1) | 16 (17.8) |
| III | 11 (17.2) | 8 (30.8) | 19 (21.1) |
| IV | 34 (53.1) | 7 (26.9) | 41 (45.6) |
| unknown (not IV) | 1 (1.6) | 1 (3.8) | 2 (2.2) |
| Line of therapy, n (%) | | | |
| First line | 38 (59.3) | 15 (57.7) | 53 (58.9) |
| Second line | 13 (20.3) | 4 (15.4) | 17 (18.9) |
| 3-5 line | 10 (15.6) | 6 (23.1) | 16 (17.8) |
| ≥6 line | 3 (4.7) | 1 (3.8) | 4 (4.4) |
| Other comorbidities, n (%) ^b | | | |
| Arterial hypertension | 29 (45.3) | 9 (34.6) | 38 (42.2) |
| Coronary heart disease | 8 (12.5) | 2 (7.7) | 10 (11.1) |
| Other cardiomyopathy | 2 (3.1) | 3 (11.5) | 5 (5.6) |
| Cerebrovascular disease/peripheral vascular disease | 6 (9.4) | 2 (7.7) | 8 (8.9) |
| Chronic pulmonary disease | 2 (3.1) | 1 (3.8) | 3 (3.3) |
| Diabetes | 8 (12.5) | 6 (23.1) | 14 (15.6) |
| Other endocrine disorder | 12 (18.8) | 5 (19.2) | 17 (18.9) |
| Hepatic disease | 6 (9.4) | 3 (11.5) | 9 (10.0) |
| Renal disease | 5 (7.8) | 5 (19.2) | 10 (11.1) |
| Rheumatic disease | 2 (3.1) | 3 (11.5) | 5 (5.6) |
| No comorbidities | 4 (6.3) | 0 (0) | 4 (4.4) |
| BMI, n (%) | | | |
| <18.5 | 1 (1.6) | 2 (7.7) | 3 (3.3) |
| ≥18.5 to <25.0 | 29 (45.3) | 8 (30.8) | 37 (41.1) |
| ≥25.0 to <30.0 | 13 (20.3) | 7 (26.9) | 20 (22.2) |
| ≥30.0 | 8 (12.5) | 4 (15.4) | 12 (13.3) |
| NA | 13 (20.3) | 5 (19.2) | 18 (20.0) |
| Treatment, n (%) | | | |
| PD-1/PD-L1 mono | 24 (37.5) | 11 (42.3) | 35 (38.9) |
| CTLA-4 + PD-1/PD-L1 | 9 (14.1) | 6 (23.1) | 15 (16.7) |
| CTLA-4 mono | 1 (1.6) | 1 (3.8) | 2 (2.2) |
| PD-1/PD-L1 + CTX | 5 (7.8) | 3 (11.5) | 8 (8.9) |
| PD-1/PD-L1 + TKI | 6 (9.4) | 3 (11.5) | 9 (10.0) |
| PD-1/PD-L1 + VEGF | 9 (14.1) | 2 (7.7) | 11 (12.2) |
| PD-1/PD-L1 + RTX | 2 (3.1) | - | 2 (2.2) |
| PD-1/PD-L1 + other | 8 (12.5) | - | 8 (8.9) |

^aOthers include ampullary carcinoma, adrenocortical carcinoma, cholangiocarcinoma, carcinoma of unknown primary, dermal squamous cell carcinoma, esophageal squamous cell carcinoma, head and neck mucosal melanoma, kidney renal papillary cell carcinoma, lung adenocarcinoma, neuroendocrine tumor, oral squamous cell carcinoma and renal cell carcinoma. ^bNumber of patients with comorbidity listed. Patients can have multiple comorbidities. H&N, head and neck; EG, esophagogastric; UICC, Union for International Cancer Control; BMI, body mass index; NA, not available; CTX, chemotherapy; TKI, tyrosine kinase inhibitor; VEGF, vascular endothelial growth factor antibody; RTX, radiotherapy; -, not applicable.

(n = 15) and a combination of anti-PD-1/PD-L1 with anti-VEGF (n = 11) (Table 1 and Fig. 1d). Despite the limited patient sizes of our cohorts, vaccinated and unvaccinated patients showed similar clinical characteristics such as sex, age, tumor type, stage, comorbidities,

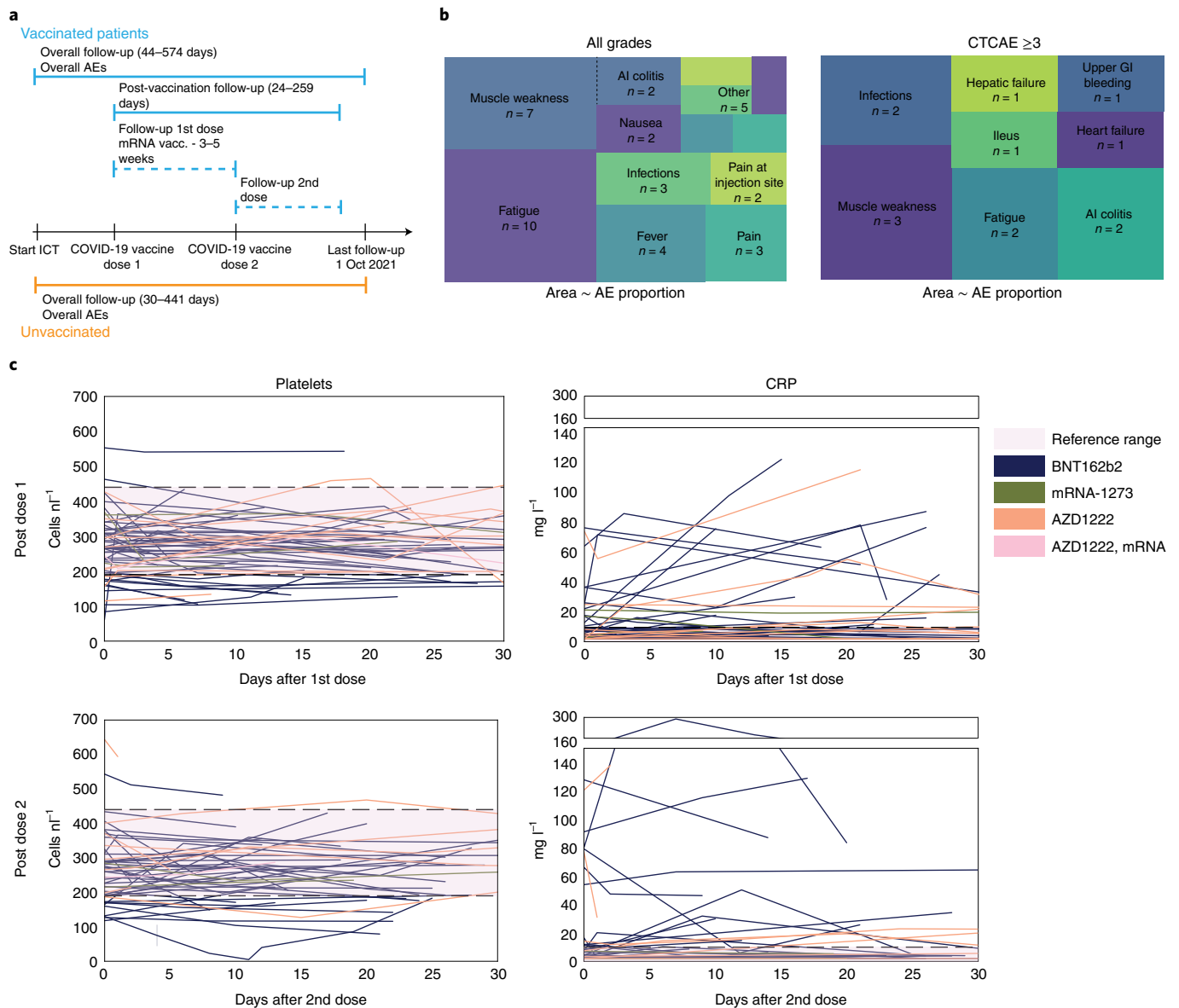


Fig. 2 | Early adverse events after COVID-19 vaccination under immune-checkpoint therapy. **a**, Schematic timeline depicting the start and duration of follow-up and vaccination time points of vaccinated and unvaccinated patients. **b**, Tree maps visualizing the proportion and the numbers of all and grade ≥ 3 AEs up to 4 weeks after vaccination in vaccinated patients ($n = 64$). In tree map for all AE: others ($n = 5$) include vomiting ($n = 1$), ileus ($n = 1$), upper GI bleed ($n = 1$), hepatic failure ($n = 1$) and heart failure ($n = 1$); pain ($n = 3$) includes headache ($n = 2$) and arthralgia ($n = 1$); infections ($n = 3$) include *C. difficile* infection ($n = 1$), *E. coli* sepsis ($n = 1$) and herpes simplex reactivation ($n = 1$). In tree map for grade ≥ 3 AEs: infections ($n = 2$) include *C. difficile* infection ($n = 1$) and *E. coli* sepsis ($n = 1$). **c**, Line-plots indicating platelet counts ($n = 61$, left) and CRP ($n = 55$, right) either after the first vaccine dose (top) or second vaccine dose (bottom). Reference ranges are indicated in pink shading. Lines are colored according to the vaccination schema used with the color code indicated below. NA, not available.

therapy regimen and line of therapy (Table 1) and were hence deemed suitable for further comparisons.

Clinical CRS is infrequent after COVID-19 vaccination. To estimate safety of COVID-19 vaccination under ICI therapy, we analyzed early AEs from the first dose until 4 weeks after the second COVID-19 vaccination dose (Fig. 2a, Table 2 and Supplementary Table 2); however, it must be noted that this study was not powered to assess the exact frequency of AEs after vaccination. While fewer early local AEs such as pain at the injection site ($n = 2$, 3.1%) were reported in our cohort, early systemic AEs were comparable to reported AEs in patients with cancer, including patients under ICI therapy^{14,15}. The most common systemic AEs included fatigue

($n = 10$, 15.6%), muscle weakness ($n = 7$, 10.9%) and fever ($n = 4$, 6.3%) (Fig. 2b and Table 2). Six patients (9.4%) were hospitalized due to grade ≥ 3 AEs and two of these patients died (3.1%) (Fig. 2b). These patients are described in detail in the Supplementary Note.

One patient who received the BNT162b2 vaccine was admitted after the first COVID-19 vaccination for autoimmune colitis, which resolved under intravenous (i.v.) glucocorticoids with subsequent oral tapering (Supplementary Note). The patient was also admitted with grade 4 anemia due to esophageal varices bleeding after the second COVID-19 vaccination and recovered quickly under high-dose proton pump-inhibitor therapy. During this stay the patient also experienced a brief febrile (38–39°C) episode of 2 d for which no infectious focus could be established. Although the patient did not

Table 2 | Early adverse events after COVID-19 vaccination (≤4 weeks)

| AE | Any grade | Grade ≥3 |
|---------------------------------|-----------|-----------|
| Any AE, n (%) | 39 (60.9) | 8 (12.5) |
| No AE, n (%) | 25 (39.1) | 56 (87.5) |
| AET, n (%) | | |
| Fatigue | 10 (15.6) | 2 (3.1) |
| Pain at injection site | 2 (3.1) | 0 (0.0) |
| Muscle weakness | 7 (10.9) | 3 (4.7) |
| Fever | 4 (6.3) | 0 (0.0) |
| Infections ^a | 3 (4.7) | 2 (3.1) |
| Nausea | 2 (3.1) | 0 (0.0) |
| Pain ^b | 3 (4.7) | 0 (0.0) |
| Vomiting | 1 (1.6) | 0 (0.0) |
| Upper GI bleeding | 1 (1.6) | 1 (1.6) |
| Ileus | 1 (1.6) | 1 (1.6) |
| AI colitis | 2 (3.1) | 2 (3.1) |
| Hepatic failure | 1 (1.6) | 1 (1.6) |
| Heart failure | 1 (1.6) | 1 (1.6) |
| CRS grade ≥2 | 0 (0) | 0 (0) |
| Laboratory abnormalities, n (%) | | |
| Anemia | 7 (10.9) | 1 (1.6) |
| Thrombocytopenia | 8 (12.5) | 1 (1.6) |
| Bilirubin increase | 8 (12.5) | 0 (0) |
| Creatinine increase | 6 (9.4) | 1 (1.6) |
| Alanine transaminase increase | 1 (1.6) | 1 (1.6) |
| Aspartate transaminase increase | 1 (1.6) | 1 (1.6) |
| Death, n (%) | 2 (3.1) | |

^aInfections, *C. difficile* diarrhea (n=1), herpes simplex reactivation (n=1) and *E. coli* sepsis (n=1)
^bPain, headache (n=2) and arthralgia (n=1). GI, gastrointestinal; AI, autoimmune.

show hypotension or hypoxia and recovered after 2 d on ampicillin/sulbactam, we cannot fully exclude the possibility that vaccination contributed to this febrile episode. The second patient experienced grade 3 increase of transaminases under pembrolizumab + axitinib and the mRNA-1273 vaccine, which normalized within 3 weeks after initial i.v. methylprednisolone and subsequent oral glucocorticoid tapering (Supplementary Note). The third patient already exhibited grade 2 diarrhea before BNT162b2 vaccination which worsened to grade 3 2 weeks after vaccination (Supplementary Note). Multiplex-PCR analyses of stool showed *Clostridium difficile* and symptoms improved after therapy with i.v. fluids and antibiotics. The fourth patient received the BNT162b2 vaccine and was admitted due to grade 3 diarrhea for which no infectious cause could be determined and was therefore deemed to be ICI-related (Supplementary Note). Symptoms resolved under i.v. fluids and corticosteroids with oral tapering. One patient died from hepatic failure after computed tomography (CT)-confirmed fulminant hepatic disease progression causing cholestasis (Supplementary Note). Finally, one patient with a history of combined severe aortic stenosis (0.8 cm² aortic valve area) and aortic insufficiency, who had paused all cardiac medication against the treating physician's advice, died at home after cardiac decompensation with pleural effusion and lower limb edema after AZD1222 administration (Supplementary Note).

We observed fever in several patients after vaccination (6.25%), which has also been observed in phase 3 trials leading to vaccine

approval in patients without cancer (Fig. 2b and Table 2)^{7,9,16}. We cannot fully exclude the possibility of grade I CRS in these patients, which can manifest as fever alone according to the ASTCT¹¹ or CTCAE v.5.0 criteria predefined in the study protocol; however, we observed no hypotension or hypoxia in any febrile patient and hence no CRS ≥ grade II (Fig. 2b and Supplementary Tables 2 and 3). Despite this observation, it is theoretically possible that cytokine release may have contributed to some AEs. In the above-mentioned case report, CRS was associated with thrombocytopenia and CRP increase¹³. In our cohort, only one patient experienced grade ≥3 thrombocytopenia with a platelet count of 5 nl⁻¹ 4 d after the second BNT162b2 dose (Fig. 2c). This patient had received gemcitabine and carboplatin 3 d before the event while still under prednisolone (50 mg d⁻¹) due to a grade 3 autoimmune hemolytic anemia, which started after a blood transfusion 2 months earlier. The patient was asymptomatic, afebrile and was not hospitalized. Moreover, platelet counts spontaneously normalized within 2 weeks thus making CRS unlikely (Fig. 2c). We frequently observed mild (>30 mg l⁻¹ and >1.5-fold) CRP increase after vaccination (n=22, 40% after first dose; n=17, 35% after second dose; Fig. 2c). One patient showed a severe CRP increase (80–289 mg l⁻¹) peaking 7 d after the second BNT162b2 dose (Fig. 2c). This patient was also asymptomatic, including absence of fever/hypotension or hypoxia, thus making CRS unlikely. Blood and urine cultures remained negative and CRP spontaneously dropped below 100 mg l⁻¹ within 2 weeks. Hence, we did not observe any clinically apparent CRS after COVID-19 vaccination in our cohort, suggesting that CRS may be rare in patients under ICI therapy with concurrent COVID-19 vaccination.

CRS-like cytokine release after COVID-19 vaccination. To evaluate cytokine responses indicative of CRS, we analyzed serum levels of CRS-associated cytokines in 35 patients undergoing concurrent ICI therapy and COVID-19 vaccination with a baseline sample ≤6 months before vaccination and a sample ≤6 weeks after vaccination (Fig. 3a,b and Extended Data Fig. 1). We excluded one patient who had an immune-related AE (arthritis grade 3) at baseline before vaccination.

To analyze cytokines induced by vaccination under ICI therapy, we performed pairwise correlation of all measured cytokines, which yielded four clusters of pairwise-correlated cytokine programs (colored sidebars; Fig. 3a). To assess the stability of this clustering we bootstrapped the probability of each pair of cytokines falling into the same cluster (Methods). Bootstrapping confirmed the stability of cytokine program 1, whereas the other clusters were more heterogeneous (Fig. 3b). Assessment of the log(fold change) of cytokine concentrations indicated that cytokine programs 1 and 4 were upregulated after vaccination in most patients although only program 1 was statistically significant ($P=0.0097$, $q=0.0389$ (false discovery rate)) likely due to the limited sample size and power (Fig. 3c). Program 4 ($P=0.0375$, $q=0.075$) included mediators previously described in CRS after the BNT162b2 vaccine in an anti-PD-1 treated patient with cancer such as interleukin (IL)-18 and sIL-2RA¹³. Program 1 included hallmark CRS cytokines and CRS mediators indicative of T-cell (IL-2) and myeloid cell activation (IL-6 and CXCL8 (IL-8, CCL2 and sIL-1R)); Fig. 3d and Extended Data Fig. 2). IL-6 has been linked to CRS severity in multiple studies and surpassed 50 pg ml⁻¹ (research grade measurement) in eight patients (22.2%), levels frequently observed in patients with severe COVID-19 or CAR-T-cell-induced CRS^{17–19} (Fig. 3d). Stratification by patient characteristics revealed that cytokine program 1 was predominantly upregulated after BNT162b2 vaccination and after combination immunotherapy, especially in patients with hepatocellular carcinoma treated with atezolizumab/bevacizumab (Extended Data Fig. 3); however, these changes were statistically non-significant. Most patients received the BNT162b2 vaccine and univariate linear regression suggested that these features only weakly predicted

the increase in cytokine program 1 observed in our patient cohort (Extended Data Fig. 4). To explore clinical correlates of these changes we analyzed the AEs in the ten patients with the highest induction of cytokine program 1 (fold change ≥ 1.7 ; Table 3). These patients showed some grade I AEs such as fatigue and arthralgia but no higher-grade AEs or fever, the CRS-defining symptom according to CTCAE or ASTCT (Table 3). All these patients were alive at the end of follow-up (Table 3). Overall, our results suggest induction of CRS-related cytokines as a frequent event after COVID-19 vaccination. This induction, however, does not seem to routinely result in CRS symptoms in the ICI-treated patients with cancer in our study.

Adverse events after COVID-19 vaccination under ICI. To assess whether vaccination increased the frequency of ICI-related AEs at later time points we compared AEs and hospitalization frequencies in vaccinated ($n=64$) and unvaccinated patients ($n=26$) over the entire follow-up period (Extended Data Fig. 5a and Supplementary Tables 3 and 4). We did not detect any significant differences in any grade or grade ≥ 3 AEs between vaccinated and unvaccinated patients under ICI therapy (Fig. 4a,b). One patient experienced grade 2 CRS before COVID-19 vaccination but no patient showed CRS after vaccination. Immune-related AEs were more frequent in unvaccinated patients, whereas vaccinated patients had a higher frequency of fatigue, nausea and lower grade thrombocytopenia, bilirubin increases and infections (Fig. 4a,b and Table 4); however, more vaccinated patients were hospitalized due to immune-related AEs (irAEs) (8 of 19) compared to unvaccinated patients (2 of 10; Fig. 4c). To confirm the accuracy of these comparisons, we calculated propensity scores based on age-, sex- and insurance status-matched (Extended Data Fig. 5b–d) as well as on age-, sex- and Eastern Cooperative Oncology Group (ECOG)-matched vaccinated and unvaccinated patients (Extended Data Fig. 6a–c). Again, overall and grade ≥ 3 AEs were comparable between the matched cohorts (Extended Data Figs. 5b–d and 6a–c) suggesting that it is unlikely that COVID-19 vaccination profoundly increased the incidence of severe AEs in ICI-treated patients with cancer. To further characterize the propensity for AEs in our patient cohort, we analyzed the time to first overall or time to first \geq grade 3 AE in unvaccinated and vaccinated individuals (Extended Data Fig. 7). When considering the entire period under immune-checkpoint therapy the propensity for AEs (both overall and \geq grade 3 AE) was higher in unvaccinated patients compared to vaccinated patients (Extended Data Fig. 7a). To investigate the temporal sequence of AEs and vaccination, we analyzed time to AE in the time periods before, immediately after (≤ 28 d) and at later time periods (>28 d) after vaccination (Extended Data Fig. 7b). We observed higher propensity for AEs in the immediate post-vaccination and late post-vaccination periods compared to the before-vaccination period (Extended Data Fig. 7b); however, the AE propensity in the post-vaccination periods was still lower than in unvaccinated patients. Overall, this analysis suggests that the vaccinated patient cohort had a lower AE propensity than the unvaccinated cohort across the entire ICI therapy period. This observation is unlikely to be caused by the vaccination itself but may be due to other differences in the vaccinated and unvaccinated cohort.

Starting from 15 October 2020, all patients were screened for COVID-19 at every therapy session (every 1–4 weeks) using a rapid antigen test fulfilling the quality criteria of the German Federal Institute for Vaccines and Biomedicines. We detected two COVID-19 patients in the unvaccinated cohort (7.7%, 95% CI 1.6–22.5%) who had to be hospitalized for severe pneumonia (Supplementary Table 4). One patient recovered and was able to resume therapy 6 weeks later but died 2 months after therapy resumption due to disease progression (Supplementary Table 5). The other patient died from COVID-19 pneumonia on the intensive care unit (Supplementary Table 5). We detected no COVID-19 cases in the vaccinated patient cohort, despite regular screening (95% CI 0–5.6%). Most patients were vaccinated with BNT162b2 and patient serum post-BNT162b2 vaccination neutralized SARS-CoV-2 S1 protein binding to recombinant human ACE2 in a competitive immunoassay (Extended Data Fig. 8). Hence, our results corroborate the increasing evidence that the here investigated COVID-19 vaccines have clinically meaningful activity in ICI-treated patients with cancer^{8,15}.

To explore whether vaccination status was associated with oncological outcomes, we compared overall survival of vaccinated and unvaccinated patients (Fig. 4d). Vaccinated patients showed prolonged survival compared to unvaccinated patients (HR 0.21, $P=0.002$) (Fig. 4d). This effect could not be explained by the single COVID-19 related death we observed among unvaccinated patients (Supplementary Table 5) and was stable across patient subgroups (Extended Data Fig. 9). Moreover, we confirmed this result in a Cox proportional hazards model, where vaccination status was the strongest predictor of prolonged overall survival (coefficient -1.72 95% CI -2.97 to -0.46 ; $P=0.01$) (Fig. 4e). As patients were recruited at the start of ICI therapy and not randomized to vaccination, our survival analyses may be subject to guarantee-time bias²⁰. We therefore performed a landmark analysis with the landmark set to 17 May 2020, the date of general eligibility for vaccination in the state of Baden-Württemberg (Germany). Before this landmark, high-risk populations, including patients with cancer, had prioritized access to COVID-19 vaccines and consequently 91.9% of all patients vaccinated in this study received their vaccination up to this date. We found that survival of vaccinated patients differed from non-vaccinated patients after but not before the vaccination landmark (Extended Data Fig. 10), further supporting an association of vaccination status with prolonged overall survival in our study. Hence, these data suggest an unexpected association of COVID-19 vaccination and prolonged overall survival in our patient cohort.

Discussion

In this prospectively planned cohort study, we describe a set of CRS-related cytokines commonly upregulated after COVID-19 vaccination in ICI-treated patients with cancer. None of these patients displayed symptoms of clinically relevant CRS, suggesting that CRS-associated cytokines are frequently induced but rarely symptomatic after COVID-19 vaccination under ICI therapy. Moreover, comparison to unvaccinated patients suggested that COVID-19 vaccination does not profoundly increase the rate of immune-related or

Fig. 3 | A correlated program of CRS-related cytokines is frequently upregulated after COVID-19 vaccination under immune-checkpoint therapy.

a, Heat map indicating Pearson correlation indices of \log_{10} (fold change) cytokine concentrations after COVID-19 vaccination from $n=35$ patients. Colored bars on the sides indicate clusters obtained from hierarchical clustering. **b**, Heat map indicating probability of each pair of cytokines clustering together as calculated by bootstrapping ($n=10,000$ samplings) from $n=35$ patients. Colored bars on the sides indicate clusters obtained from hierarchical clustering. **c**, Heat maps indicating \log_{10} (fold change) of cytokine concentrations after vaccination. Bar graph on the side indicates average \log_{10} (fold change) of cytokines in each row with concentrations after the first or second vaccination dose labeled according to the color code on the right from $n=35$ patients. P values (two-sided) were calculated using a Wilcoxon signed-rank test (test statistics from left to right are 231, 425, 301 and 270; Cohen's D calculated as mean fold change/s.d. fold change from left to right is 0.93, 3.22, 1.32 and 1.21). P values significant ($\alpha=0.05$) after correcting for multiple comparisons with the Benjamini-Hochberg method are indicated with an asterisk. **d**, Line-plots indicating cytokine concentrations of cytokine program 1 cytokines after vaccination from $n=35$ patients and vaccine type indicated in the color code at the bottom right.

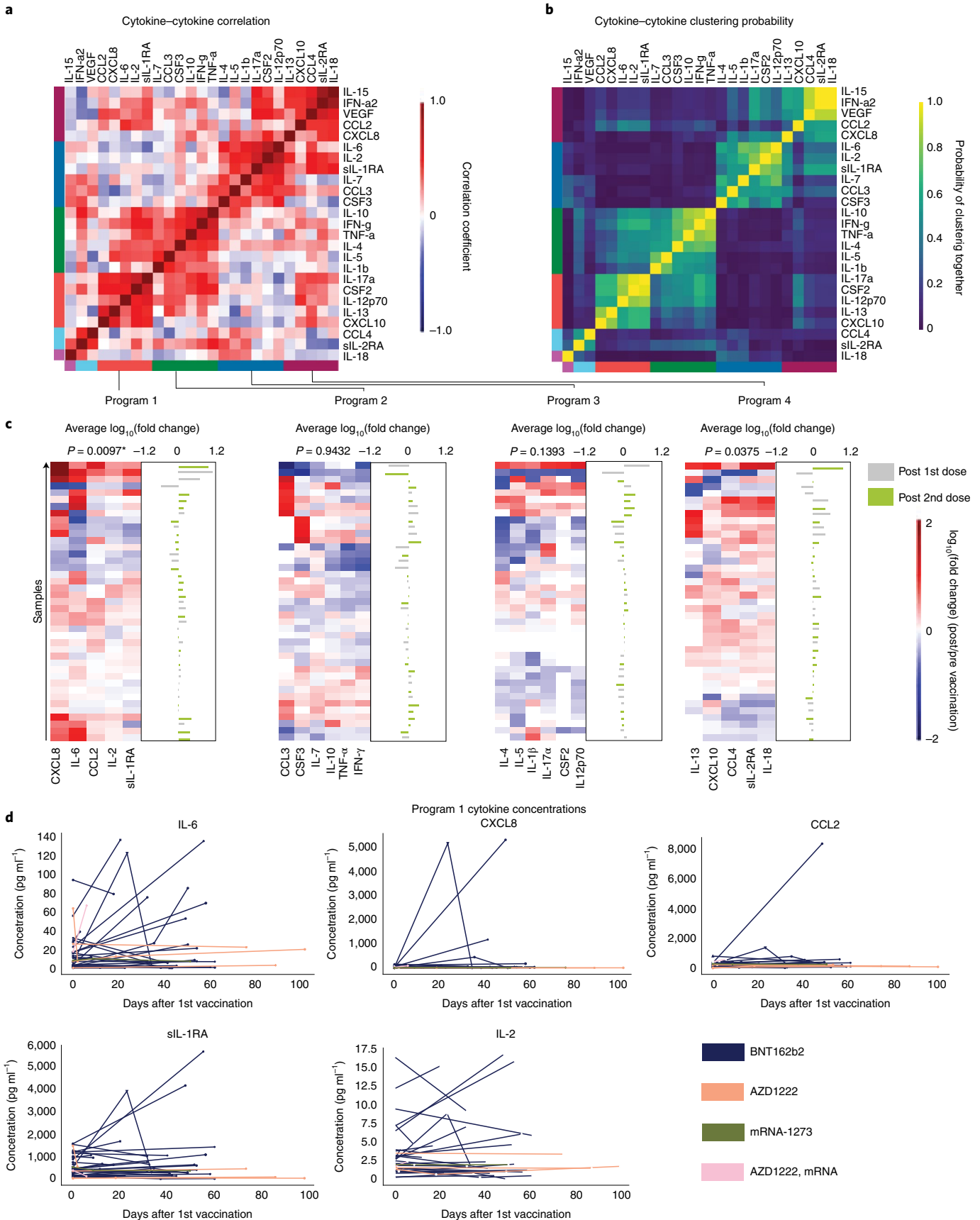


Table 3 | Adverse events in patients with highest induction of cytokine program 1

| Patient ID | Fold change cytokine | First vaccination | Second vaccination | Cytokine date | AE | AE date | CTCAE grade | Survival | Follow-up from first vaccination (days) |
|------------|----------------------|-------------------|--------------------|---------------|-------------------------|------------|-------------|----------|---|
| BWW38Q | 12.6 | 4 Jun 21 | 2 Jun 21 | 28 Jun 21 | None | NA | NA | Alive | 119 |
| OZTE2L | 9.0 | 15 Apr 21 | 27 May 21 | 04 Jun 21 | None | NA | NA | Alive | 169 |
| 2JJ523 | 4.8 | 5 May 21 | 12 Jun 21 | 10 Jun 21 | Arthralgia | 13.06.2021 | 1 | Alive | 111 |
| 1K91AN | 2.5 | 30 Apr 21 | 4 Jun 21 | 24 Jun 21 | None | NA | NA | Alive | 154 |
| EMHL0E | 2.3 | 27 May 21 | 8 Jul 21 | 20 Jul 21 | None | NA | NA | Alive | 127 |
| SO7XOB | 2.3 | 14 Apr 21 | 26 May 21 | 4 Jun 21 | Thrombocytopenia | 17.06.2021 | 1 | Alive | 170 |
| X9H3PX | 2.2 | 28 Apr 21 | 31 May 21 | 25 Jun 21 | Bilirubin increase | 04.06.2021 | 1 | Alive | 156 |
| LIK08H | 1.8 | 5 Mar 21 | 26 Mar 21 | 7 Apr 21 | Fatigue | 26.03.2021 | 1 | Alive | 210 |
| LIK08H | 1.8 | 5 Mar 21 | 26 Mar 21 | 7 Apr 21 | General muscle weakness | 26.03.2021 | 1 | Alive | 210 |
| 4WTCUA | 1.8 | 21 Apr 21 | 31 May 21 | 12 May 21 | Fatigue | 31.05.2021 | 1 | Alive | 163 |
| X65WDO | 1.7 | 12 Apr 21 | 13 May 21 | 25 Jun 21 | None | NA | NA | Alive | 172 |

Table shows AEs and CTCAE v.5.0 grading, mean fold change increase in cytokine program 1 and survival data of the ten patients with the highest mean fold change of serum cytokine levels of cytokines IL-6, CXCL8, IL-2, CCL2 and sIL-1R within 4 weeks after vaccination.

grade ≥ 3 AEs and may decrease the rate of COVID-19 infection in ICI-treated patients.

A recent case report of CRS after vaccination in a patient with colorectal cancer (CRC) treated with a PD-1 ICI highlighted the insufficient evidence regarding vaccine-related AEs in ICI-treated patients with cancer¹³. Au and colleagues presented a patient with fever, thrombocytopenia, CRP increase and elevation of several cytokines including interferon- γ , sIL-2R, IL-18, IL-16 and IL-10 after vaccination and ICI therapy compared to cytokine levels before initiation of ICI therapy and vaccination¹³. In our study we did not observe any CRS \geq grade II (95% CI 0–5.6%) after COVID-19 vaccination after both short-term (first dose until 4 weeks after second dose) and long-term (median follow-up of 24 weeks after first dose) follow-up according to the ASTCT or CTCAE v.5.0 criteria. Overall, AEs under immunotherapy were generally comparable in vaccinated (48.4% grade ≥ 3) and unvaccinated patients (69.2% grade ≥ 3). Moreover, these AE frequencies were within the range of AE frequencies reported in phase 3 clinical trials of the investigated immunotherapies (Supplementary Table 6). Thus, CRS is likely an infrequent event under combined ICI therapy and COVID-19 vaccination.

Despite the absence of clinically relevant CRS, we observed induction of a set of CRS-related cytokines after COVID-19 vaccination under ICI therapy. This included the CRS hallmark cytokine IL-6 and other CRS-related cytokines (CXCL8, IL-2, CCL2 and sIL1-RA). Induction of IL-6 has been reported after mRNA-based lipoplex tumor vaccination which was associated with generally mild and self-limiting associated symptoms²¹. Moreover, we found higher IL-2 levels after vaccination, which may be explained by T-cell activation and preferable type 1 helper T-cell polarization as shown in healthy adults vaccinated with BNT162b2 (ref. 22). Our patients also showed coordinated release of CCL2 and CXCL8 levels after COVID-19 vaccination, which can be explained by the activation of myeloid cells by the mRNA-loaded lipid nanoparticles of the BNT162b2 vaccine²³. While CCL2 and IL-2 were also reported to be induced in the above-mentioned case report of CRS in a patient with mismatch repair-deficient CRC, the CRS hallmark cytokines IL-6 and CXCL8 levels remained largely constant in this patient¹³. Our study did not include a CRC or mismatch-repair-deficient patient who received COVID-19 vaccination. It is possible that the clinical course observed by Au et al. is a CRC or mismatch-repair-deficiency-specific effect given the distinct T-cell inhibitory mechanisms in these tumors, which may render T cells more responsive to PD-1 disinhibition^{13,24}.

Notably, one patient in our study experienced grade 2 CRS before any COVID-19 vaccination was administered, highlighting that CRS can occur independently of vaccination under ICI therapy and may not necessarily be vaccine-related. This is particularly important in patients with cancer in a palliative setting with limited treatment options, as CRS treatments such as glucocorticoids may impair ICI efficacy and deprive patients of an important treatment option^{25,26}. Our results suggest that CRS-related cytokines are commonly induced after COVID-19 vaccination and are not sufficient to establish the diagnosis of CRS. Clinically relevant CRS should therefore be diagnosed in symptomatic patients after an exhaustive differential diagnosis.

Two cases of severe COVID-19 (95% CI 1.6–22.5%) occurred in our unvaccinated cohort but none in our vaccinated patients. We observed induction of neutralizing antibodies after vaccination, thus corroborating current evidence that COVID-19 vaccines may have meaningful activity in ICI-treated patients with cancer⁸.

Vaccinated patients also showed increased overall survival in our study and vaccination status was an independent predictor of overall survival in a Cox proportional hazards model. A similar observation was reported in influenza-vaccinated patients with cancer who showed prolonged overall survival under ICI compared to unvaccinated patients²⁷. In our study, this result was further supported by landmark analysis making guarantee-time bias an unlikely but not impossible explanation for this observation. Moreover, the prolonged overall survival in vaccinated patients cannot be explained by COVID-19-related mortality of unvaccinated patients alone. In unvaccinated patients only one in nine deaths was caused directly by COVID-19 infection and one death occurred due to tumor progression shortly after COVID-19 infection. As patients underwent regular rapid antigen-testing (q1w-q4w) it is unlikely that we missed a relevant number of COVID-19 cases. It is possible that the small sample size of our heterogenous cohort may have skewed the survival analysis despite the similarity of vaccinated and unvaccinated patients in many clinical covariates. Our results should therefore be validated in larger patient cohorts. Alternatively, patients with worse disease status and symptoms may be more hesitant and less likely to get vaccinated. This hypothesis is supported by the fact that unvaccinated patients experienced numerically more severe AEs. This observation may also be a result of increased health awareness or higher compliance regarding oncological therapy in vaccinated patients, an outcome that we did not assess in this study. Another possible explanation is that the cytokine boost induced by

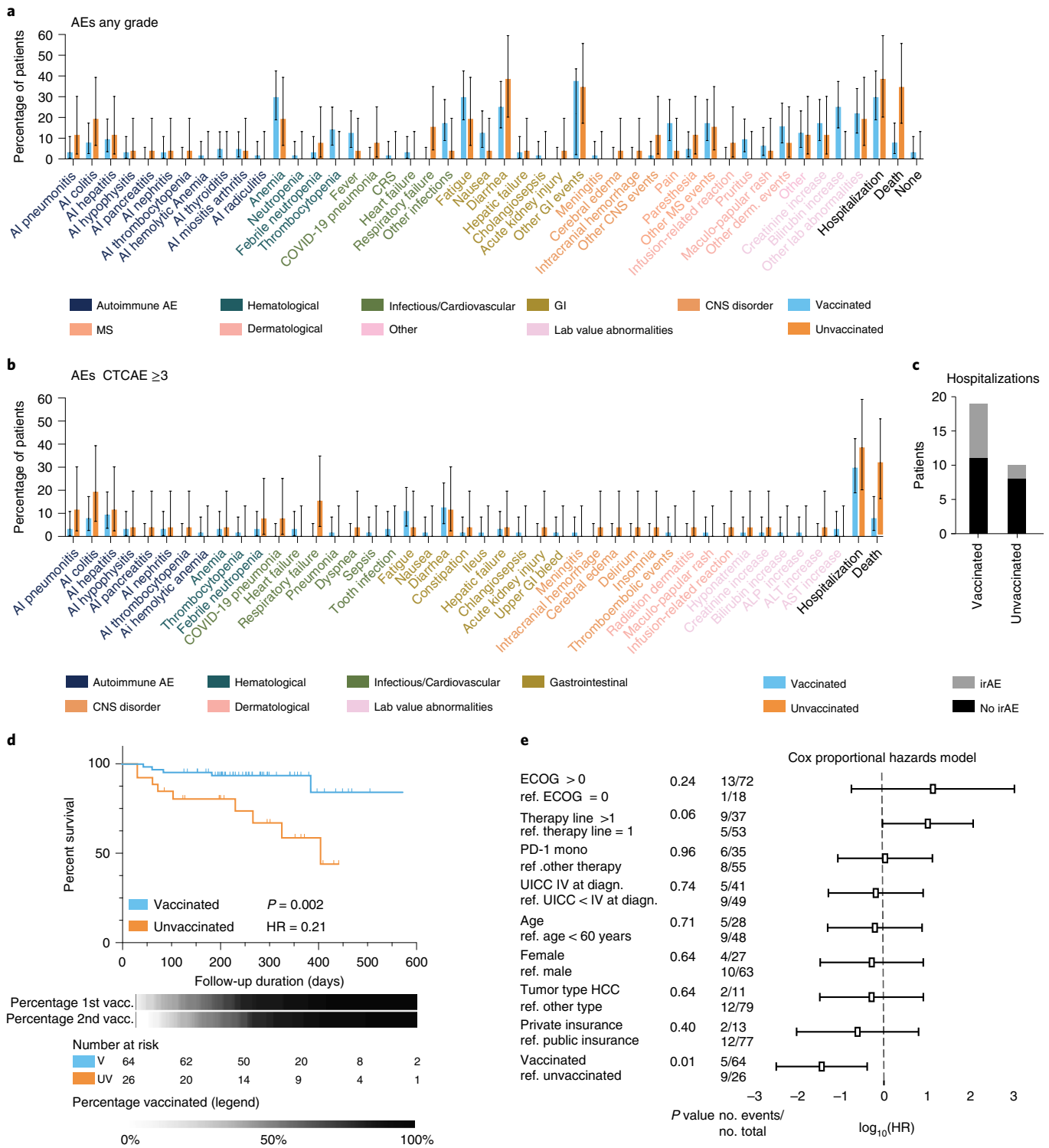


Fig. 4 | Comparable adverse events and prolonged overall survival in COVID-19-vaccinated immune-checkpoint therapy-treated patients with cancer. **a,b**, Grouped bar plots indicating the frequency and error bars the 95% CI of overall AE (**a**) or grade ≥ 3 AEs (**b**) under ICI therapy in vaccinated ($n=64$) and unvaccinated ($n=26$) patients. This is proportional data and the CI is asymmetric and the center is the bar. **c**, Total number of hospitalizations due to irAEs and other AEs in vaccinated and unvaccinated patients (as listed in Supplementary Table 4) in vaccinated ($n=19$) and unvaccinated ($n=10$) patients. **d**, Kaplan-Meier curve indicating overall survival probability of vaccinated ($n=64$) and unvaccinated ($n=26$) patients under ICI therapy. P values (two-sided, test statistic 9.345) and hazard ratios (95% CI = 0.07–0.69) were calculated using a log-rank test. Grey gradient bars indicate the proportion of patients who received the first or second vaccination dose over time with the timeline indicated above and color legend indicated below. **e**, Forest plot indicating the results of the Cox proportional hazards model of $n=90$ patients with squares indicating the $\log_{10}(\text{HR})$ and whiskers indicating the 95% CI. P values (two-sided) were not corrected for multiple comparisons and number of events are indicated on the left. HR, hazard ratio; CNS, central nervous system; MS, musculoskeletal.

Table 4 | Immune-related adverse events under immunotherapy in vaccinated and non-vaccinated patients

| Characteristic, n (%), 95% CI) | Vaccinated (n = 64) | Unvaccinated (n = 26) |
|----------------------------------|-----------------------------|-----------------------------|
| Any AE (irAE + non-irAE) | 62 (96.9, 89.2–99.6) | 25 (96.2, 80.4–1.0) |
| Grade ≥ 3 (irAE + non-irAE) | 31 (48.4, 35.8–61.3) | 18 (69.2, 48.2–85.7) |
| AI pneumonitis | 2 (3.1, 0.4–10.8) | 3 (11.5, 2.4–30.2) |
| AI colitis | 5 (7.8, 2.6–17.3) | 5 (19.2, 6.6–39.4) |
| AI hepatitis | 6 (9.4, 3.5–19.3) | 3 (11.5, 2.4–30.2) |
| AI hypophysitis | 3 (4.7, 1.0–13.1) | 1 (3.9, 0.1–19.6) |
| AI pancreatitis | 0 (0.0, 0.0–5.6) | 1 (3.9, 0.1–19.6) |
| AI nephritis | 2 (3.1, 0.4–10.8) | 1 (3.9, 0.1–19.6) |
| AI thrombocytopenia | 0 (0.0, 0.0–5.6) | 1 (3.9, 0.1–19.6) |
| AI hemolytic anemia | 1 (1.6, 0.0–8.4) | 0 (0.0, 0–13.2) |
| AI thyroiditis | 3 (4.7, 1.0–13.1) | 0 (0.0, 0–13.2) |
| AI myositis/arthritis | 3 (4.7, 1.0–13.1) | 1 (3.9, 0.1–19.6) |
| AI radiculitis | 1 (1.6, 0.0–8.4) | 0 (0.0, 0–13.2) |

Table indicating absolute numbers, frequencies and 95% CI of irAEs. The study has not been powered to evaluate the exact frequency of rare irAEs under ICI therapy and COVID-19 vaccination. The irAEs that are numerically more frequent in either the vaccinated or non-vaccinated group are marked in bold font.

vaccination may have reinforced antitumor immunity. Specifically, IL-2 induction, as observed in our vaccinated patients, can break ICI resistance in subcutaneous murine models²⁸. Despite the favorable survival data for our vaccinated patients, it should be noted that two patients died within 4 weeks after vaccination. It seems unlikely that these were causally related to the vaccine given plausible alternative explanations, namely computed tomography-confirmed hepatic tumor progression in one patient and severe aortic stenosis in combination with abrupt discontinuation of all cardiac medication by the other patient. However, cardiovascular events after COVID-19 vaccinations have been reported and should be closely monitored²⁹. Overall, the tested COVID-19 vaccines were linked to favorable outcomes in our study, may have meaningful clinical activity in ICI-treated patients with cancer and warrant validation in larger ICI-treated patient cohorts.

Despite these insights, our study also has several limitations which should be considered in its interpretation. This is a cohort study and patients were not randomly assigned to vaccination. This led to a difference in AE propensity before vaccination as compared to unvaccinated patients, which given the observational nature of the study might have biased assessment of post-vaccination AEs. AEs and cytokine levels under SARS-CoV-2 vaccination were not the primary end point of this study; therefore, sample size was not optimized for these end points and our trial was not powered to estimate the exact frequency of rare AEs under ICI therapy and COVID-19 vaccination. Larger studies are necessary to determine this, although even phase 3 trials are often not powered for this comparison³⁰. Moreover, AEs were assessed upon presentation at our day clinic every 1–6 weeks and not at a standardized early time point, as performed for randomized controlled vaccination trials⁹. While serious AEs were generally reported instantly, lower grade AEs may be underreported due to recall bias. Finally, all serum cytokine and antibody titer analyses were research grade and absolute concentrations from this study should not be used to establish clinical diagnoses. It is important to note that these drawbacks, such as small sample size and lack of randomization, also apply to other studies that have analyzed COVID-19 vaccinations in patients with cancer^{8,14,15}. Strengths of our analysis include

the prospective design, prospective recruitment of most patients, long-term follow-up, broad array of cancer types and combination immune-checkpoint therapies.

In summary, our data indicate that induction of CRS-related cytokines after COVID-19 vaccination is common in ICI-treated patients with cancer, but is generally not associated with clinical CRS symptoms meeting current CRS diagnostic criteria. Hence, cytokine induction is not sufficient to diagnose CRS in these patients. Our data warrant validation in larger cohorts to define the exact frequencies of CRS and other AEs in ICI-treated patients with cancer receiving COVID-19 vaccination. Overall, our study supports current clinical practice of COVID-19 vaccination in patients with cancer under ICI therapy.

Methods

Clinical trial. The presented trial was conducted in accordance with the declaration of Helsinki in its current edition and all relevant ethical regulations. The trial received institutional ethics review board approval at Ethics Commission I Medical Faculty Heidelberg, Heidelberg University (S-373/2020, S-207/2005) and Ethics Commission II Medical Faculty Mannheim, Heidelberg University (2021–567). Trial personnel were subject to medical confidentiality (paragraph 9 (Muster-)Berufordnung für die in Deutschland tätigen Ärztinnen und Ärzte), the General Data Protection Regulations (DSGVO) and the Data Protection Act of the state of Baden-Württemberg (LSDG).

Patients presented in this study are part of the exploration cohort of a prospectively registered cohort study (DRKS00022890). The exploration cohort consisted of 220 patients of whom 166 were recruited prospectively and 54 retrospectively. Of these patients, 29 patients with dermatological cancers were also included in a retrospective survey study at our center³¹. All these patients are part of the here-reported prospectively registered trial and gave written informed consent for the investigations. For prospectively recruited patients this consent was study specific and for retrospectively recruited patients the consent was general but included the here-reported investigations. The trial including both prospective and retrospective patients has been approved by the Ethics Commission I Medical Faculty Heidelberg, Heidelberg University (S-373/2020 and S-207/2005) and Ethics Commission II Medical Faculty Mannheim, Heidelberg University (2021–567). Patients consented for data to be stored for up to 10 years after trial completion by Heidelberg University Hospital. All patients had been provided with contact numbers to request data deletion and their rights within the DSGVO as well as contact information of relevant oversight authorities. None of the here-reported patients requested data deletion, modification or restriction of its use and no patient withdrew consent. Patients consented that their data may be published in pseudonymized form and consented that after publication, deletion of the published data and analyses is no longer possible.

Adult patients with advanced solid tumors starting a new cancer immunotherapy either as mono- or combination therapy, excluding adoptive cell therapies were eligible for inclusion. Written informed consent, hemoglobin levels $\geq 80 \text{ g l}^{-1}$ when additional blood samples were obtained and measurable disease according to RECIST 1.1 were obligatory requirements for inclusion. Patients received no compensation for participating in this trial. This is a single-arm cohort study and hence no randomization was performed. Patients were followed up at least every 1–6 weeks depending on the treatment regimen. AEs were continuously retrieved from electronic patient health records and graded according to CTCAE v.5.0 as per the trial protocol (German Clinical Trial Register DRKS00022890). Additionally, we applied the ASTCT 2019 criteria for CRS, which are more specific to immunotherapies (developed for adoptive cell therapies) but otherwise are very similar to CTCAE v.5.0. In contrast to previous CTCAE criteria neither the CTCAE v.5.0 nor the ASTCT criteria include organ toxicities in CRS diagnosis. The CTCAE v.5.0 and the ASTCT 2019 criteria require fever, hypoxia or hypotension as the defining feature of clinical CRS¹¹. These criteria are likely imperfect and may require adaptation in the future. One example is that fever is also sufficient to diagnose CRS grade I according to these criteria but as noted by June and Fajgenbaum¹² is also part of many appropriate clinical reactions that should not be diagnosed as CRS. We therefore only considered CRS grade $\geq \text{II}$ as clinically relevant.

Other metadata collected included age at time of written informed consent, sex, tumor type, stage and histology, mutational status, sites of metastases, history of tobacco use, pre-existing health conditions, concurrent medication and survival. Pre-existing health conditions were obtained from electronic patient records and defined according to the Side Effect Resource (SIDER v.4.1: <http://sideeffects.embl.de>). Every week to every four weeks, patients also received regular clinical laboratory tests, including creatinine, bilirubin, CRP, hemoglobin, platelet and leukocyte counts. Additionally, patients received longitudinal blood samples for cytokine measurements before the start of therapy, within 1–7 weeks after therapy initiation and every 8–12 weeks under immunotherapy. COVID-19 vaccination status was assessed during regular follow-up. Patients did not undergo any additional screening for determination of vaccination status.

The primary outcome measure of the trial was prediction of radiological response, which will be reported elsewhere. Secondary outcome measures included the serum proteome and peripheral blood immune cell composition overall, grade 3 AEs as well as progression-free and overall survival. Patient health information is pseudonymized.

Analysis of serum cytokines and neutralizing antibodies. Blood was collected either peripherally through venipuncture or via a central port catheter in coagulation matrix containing serum tubes (no. 01.1602, Sarstedt) from live patients with cancer. Clinical characteristics and tumor types are indicated in Table 1. Samples were kept at room temperature until preparation (generally <6 h, but always <24 h). Samples were prepared at the National Center for Tumor Diseases (NCT) Liquidbank biobank using a standard operating procedure: for serum preparation, tubes were centrifuged at 2,500g for 10 min at room temperature and the upper phase was transferred into 500- μ l aliquots and stored at -80°C . For both cytokine and antibody analysis we only selected patients with baseline samples obtained within 6 months before vaccination. For cytokine analysis we selected all samples obtained up to 6 weeks after vaccination. For antibody analysis we selected all samples until the end of follow-up. Samples were analyzed at NCT Heidelberg or the German Cancer Research Center (DKFZ) immediately after thawing; no shipping was required. Reporting was conducted in accordance with BRISQ criteria³².

Serum samples were thawed and immediately analyzed in duplicate using the Legendplex Cytokine Storm Panel 1 (AB_2895549 (antibodyregistry.org), 741091, BioLegend), Cytokine Storm Panel 2 (AB_2895550 (antibodyregistry.org), 741142, BioLegend) or SARS-CoV-2 Neutralizing Antibody Assay (AB_2895551 (antibodyregistry.org), 741127, BioLegend) according to manufacturer's instructions and analyzed on a BD FACS Canto II flow cytometer (BD) using the BD FACS DIVA v.8.0 software (BD). In brief, patient serum was diluted to 1:2 or to 1:100 of the initial concentration for the cytokine multiplex and neutralizing antibody assay, respectively. Diluted serum, standard, assay buffer, matrix, antibody-coupled capture beads and biotinylated detection antibodies were transferred to a 96-well V-bottom microplate. After incubation and washing streptavidin-PE was added to each well and cells were transferred to flow cytometry tubes and acquired using a FACS Canto II (BD). The gating for flow cytometry analysis is depicted in Extended Data Fig. 1. Analyte concentrations were interpolated from a standard curve using 5 parameter logistic regression using Legendplex Software v.2021.07.01 (BioLegend). Cytokine concentrations below the lower limit of detection were set to 0.

General data analysis. All data analysis was performed using Python 3 in a Jupyter notebook or GraphPad Prism v.9.2.0 (GraphPad Software). All computer code is provided under GitHub at https://github.com/wallet-maker/ANTICIPATE_COVID-19 and <https://zenodo.org/record/6544522#.YoYKBXXMLcs>. Plotting was conducted using the Matplotlib (v.3.4.3) and Seaborn (v.0.11.2) packages. Other package versions included mgau (v.0.2.5), pandas (v.0.23.4), squarify (v.0.4.3), lifelines (v.0.26.4), statsmodels (v.0.10.2), numpy (v.1.19.5), mpmath (v.1.2.1), scipy (v.1.4.1), pymatch (v.0.3.4) and Jupyter (v.1.0.0). Plots were arranged using Adobe Illustrator 2021 (v.25.2.2, Adobe).

Bootstrapping cytokine-cytokine clustering probabilities. We transformed cytokine concentrations according to the following formula $c_i = \log_{10}(c + 1)$ with c_i as the log₁₀-transformed cytokine concentration and c as the raw cytokine concentration in pg ml^{-1} for all vaccinated patients. We then normalized all post-vaccination log₁₀-transformed concentrations by subtracting the respective log₁₀-transformed cytokine concentrations of the baseline sample. Based on these normalized concentrations, we then calculated a Pearson cytokine-cytokine correlation matrix. We then used the correlation distances as an input for the `scipy.cluster.hierarchy.linkage` function with the unweighted pair group method with arithmetic mean, to obtain the row and column linkages and transformed these into flat clusters by applying `scipy.cluster.hierarchy.fcluster` function using a cophenetic distance of 0.75.

We sampled the normalized log₁₀-transformed cytokine concentration dataframe object with replacement with the same sample size as the initial dataframe and repeated the above-mentioned procedure to obtain flat clusters. This sampling and clustering was repeated $n = 10,000$ times. For each pair of cytokines we then counted their co-occurrence in a cluster and summed the values for all 10,000 separate clusterings dividing the counts for each pair of cytokines by 10,000 to obtain an approximation of the probability for each pair of cytokines to fall into the same cluster.

Time-to-event analysis. Survival time or time to first overall or first CTCAE v.5.0 grade ≥ 3 adverse event was analyzed by Kaplan-Meier curves and log-rank tests (Mantel-Cox) using GraphPad Prism and the lifelines package (v.0.26.4). A Cox proportional hazards model was calculated using the lifelines package. We inspected the Kaplan-Meier curves and did not see any obvious violation of the proportional hazards assumption; however, when formally testing the proportional hazards assumption using the `check_assumptions` function in the lifelines packages the 'age' variable violated this assumption when used on a continuous level. We therefore stratified patients into >60 and ≤ 60 years of age at inclusion.

To gauge the effect of vaccination on AEs we calculated Kaplan-Meier statistics and event rates (events per days at risk) for different intervals: over the entire observation period (for vaccinated and unvaccinated patients), for vaccinated patients before vaccination, for the first 28 d after the first vaccination dose and for >28 d after the first vaccination dose until the end of follow-up. We did not perform time-to-event analysis for irAEs because of the limited power of this analysis. Using the lifelines package, we also calculated a Cox proportional hazards model using the variables indicated in Fig. 4d. When no events were observed in one group we reported hazard ratios using the Mantel-Hanszel method implemented in GraphPad Prism v.9.2.0. Otherwise, we used the log-rank method implemented in GraphPad Prism v.9.2.0.

Landmark analysis. We performed a landmark analysis for overall survival before or after the landmark of all vaccinated and unvaccinated patients. The landmark was set as 17 May 2020, which was the date of general eligibility for COVID-19 vaccination in the state of Baden-Württemberg, Germany (press release of the Ministry of Social Affairs, Health and Integration of the state of Baden-Württemberg, Germany, 12th May 2021: <https://sozialministerium.baden-wuerttemberg.de/de/service/presse/pressemitteilung/pid/priorisierung-in-arztpraxen-ab-17-mai-fuer-alle-impfstoffe-aufgehoben/>). Patients with cancer had prioritized access to COVID-19 vaccines before this landmark and consequently 91.9% of all patients vaccinated at some point in this study were vaccinated until this date. To assess overall survival after the landmark, patients not vaccinated up to that date were counted as unvaccinated as required in landmark analysis. *P* values were calculated using log-rank tests.

Propensity score matching. Propensity score matching was performed using the `pymatch` package (v.0.3.4) and the exact procedure is outlined in the publication describing the package³³. In brief, a linear regression model is fitted using either $\text{ECOG} \in \{ \leq 1, > 1 \}$, $\text{age} \in \text{positive integers}$ and $\text{sex} \in \{ \text{male, female} \}$ or private insurance status $\in \{ \text{true, false} \}$, $\text{age} \in \text{positive integers}$ and $\text{sex} \in \{ \text{male, female} \}$ as $k = 3$ independent variables per model. The propensity scores are defined as $\pi_i = \pi(X_i) = \Pr(T_i = 1 | X_i)$ with $X_i = (X_{i1}, X_{i2}, X_{i3}, \dots, X_{ik})$ being a vector of k features for each patient i and T_i the class membership of each patient with $T_i = 1$ if the patient was vaccinated and $T_i = 0$ if the patient was unvaccinated. The logistic regression model was defined as $\log(\pi_i / (1 - \pi_i)) = X_i \beta + \epsilon_i$, $i = 1, 2, \dots, n$.

Based on these propensity scores we assigned each unvaccinated patient a vaccinated counterpart with replacement. This led to partly efficient matching, defined as a reduction in the age and sex imbalance of the vaccinated and unvaccinated cohorts (Extended Data Figs. 5b and 6b). We did not include other variables in the calculation of propensity score because they led to perfect separation. We then compared AEs occurring under ICI therapy in unvaccinated and matched vaccinated patients.

Statistics and reproducibility. The study size was defined by sample size estimation based on the primary outcome parameter (radiological response) as outlined in the study protocol. Briefly, an area under the curve (AUC) > 0.78 for predicting radiological response was chosen as a clinically relevant threshold based on current literature. We used published data to model a receiver operator curve (sensitivity versus $1 - \text{specificity}$) and based on this, calculated AUC confidence intervals for different patient numbers assuming a response rate of 10%. A patient number of $n = 200$ resulted in a lower limit of $\text{AUC} = 0.782$ we estimated a dropout of 10%, resulting in a total of 220 patients for the training and 220 patients for the testing cohort. For the here-reported exploratory study outcomes, no statistical method was used to predetermine sample size. We excluded six patients who were fully vaccinated before the start of immunotherapy because these patients would have confounded the interpretation of study results. For the cytokine analysis, we excluded one additional patient who had an irAE at baseline before vaccination. Cytokine concentrations were measured in technical duplicate in three independent experiments with different patient subgroups (outlined in the provided code) with similar results for all these subgroups. Antibody concentrations were measured in one experiment in technical duplicate. The experiments were not randomized. Investigators retrieving patient metadata and outcome assessments were not blinded to vaccination status. The acquisition and processing of the raw cytometry data was performed by a clinician scientist who was blinded to the patients' identity and metadata and who was not involved in downstream data analysis; however, the patients' pseudonyms contained the temporal sequence of the samples.

Confidence intervals for frequencies/proportions were calculated as Clopper-Pearson intervals based on the β distribution using the `statsmodels.stats.proportion.proportion_confint` function of the `statsmodels` package (v.0.10.2). *P* values were calculated using Wilcoxon one-sample tests or Wilcoxon matched-pairs signed-rank tests for continuous/ordinal one-sample or paired two-sample data, respectively using `scipy.stats.wilcoxon` function (v.1.7.2). There was no indication for violating the assumptions of these nonparametric tests such as asymmetric difference scores. Proportional data were analyzed using a chi-squared test because its assumptions were met (two or more categorical independent variables). The Fisher's exact test could not be used because the number of patients experiencing an event (such as an AE) was unconditioned.

Survival data were analyzed using log-rank tests or Cox proportional hazards models. There was no indication that the proportional hazards assumption was violated, such as crossing of the Kaplan–Meier curves. We formally tested the proportional hazards assumption using the `check_assumptions` function of the `lifelines` Python package, which showed no indication of violation after stratifying the age variable. All *P* values are two-tailed. For cytokine data analysis *P* values were corrected for multiple comparisons with the Benjamini–Hochberg method using `R v.4.1.1` and the `p.adjust` function. For clinical data analysis we did not use multiple comparisons correction to increase our power to detect differences in vaccine-related AEs.

Reporting summary. Further information on research design is available in the Nature Research Reporting Summary linked to this article.

Data availability

Data on cytokine serum concentrations and patient metadata generated for this study are publicly available through Zenodo (<https://zenodo.org/record/6544522#.YoYUQXXMLcs>). Patient data will be anonymized 10 years after study completion. Source data for all figures are provided as Source Data files. All other data supporting the findings of this study are available from the corresponding author on reasonable request. Source data are provided with this paper.

Code availability

All custom computer code used to generate the results in this study has been deposited in a GitHub repository (https://github.com/wallet-maker/ANTICIPATE_COVID-19.git) and a Zenodo repository (<https://zenodo.org/record/6544522#.YoYUQXXMLcs>)³⁴ under an MIT license.

Received: 24 December 2021; Accepted: 16 May 2022;

Published online: 17 June 2022

References

- Russell, B. et al. Risk of COVID-19 death in cancer patients: an analysis from Guy's Cancer Centre and King's College Hospital in London. *Br. J. Cancer* **125**, 939–947 (2021).
- Trapani, D. & Curigliano, G. COVID-19 vaccines in patients with cancer. *Lancet Oncol.* **22**, 738–739 (2021).
- Ribas, A. et al. Priority COVID-19 Vaccination for Patients with Cancer while Vaccine Supply Is Limited. *Cancer Discov.* **11**, 233–236 (2021).
- Sahin, U., Karikó, K. & Türeci, Ö. mRNA-based therapeutics — developing a new class of drugs. *Nat. Rev. Drug Discov.* **13**, 759–780 (2014).
- Frenck, R.W. et al. Safety, immunogenicity, and efficacy of the BNT162b2 Covid-19 vaccine in adolescents. *New Engl. J. Med.* <https://doi.org/10.1056/NEJMoa2107456> (2021).
- Folegatti, P. M. et al. Safety and immunogenicity of the ChAdOx1 nCoV-19 vaccine against SARS-CoV-2: a preliminary report of a phase 1/2, single-blind, randomised controlled trial. *Lancet* **396**, 467–478 (2020).
- Baden, L. R. et al. Efficacy and safety of the mRNA-1273 SARS-CoV-2 vaccine. *N. Engl. J. Med.* **384**, 403–416 (2020).
- Fendler, A. et al. Adaptive immunity and neutralizing antibodies against SARS-CoV-2 variants of concern following vaccination in patients with cancer: the CAPTURE study. *Nat. Cancer* <https://doi.org/10.1038/s43018-021-00274-w> (2021).
- Polack, F. P. et al. Safety and efficacy of the BNT162b2 mRNA Covid-19 vaccine. *N. Engl. J. Med.* **383**, 2603–2615 (2020).
- Haslam, A. & Prasad, V. Estimation of the percentage of US patients with cancer who are eligible for and respond to checkpoint inhibitor immunotherapy drugs. *JAMA Network Open* **2**, e192535 (2019).
- Lee, D. W. et al. ASTCT consensus grading for cytokine release syndrome and neurologic toxicity associated with immune effector cells. *Biol. Blood Marrow Transplant.* **25**, 625–638 (2019).
- Fajgenbaum, D. C. & June, C. H. Cytokine storm. *N. Engl. J. Med.* **383**, 2255–2273 (2020).
- Au, L. et al. Cytokine release syndrome in a patient with colorectal cancer after vaccination with BNT162b2. *Nat. Med.* <https://doi.org/10.1038/s41591-021-01387-6> (2021).
- Waissengrin, B., Agbarya, A., Safadi, E., Padova, H. & Wolf, I. Short-term safety of the BNT162b2 mRNA COVID-19 vaccine in patients with cancer treated with immune checkpoint inhibitors. *Lancet Oncol.* **22**, 581–583 (2021).
- Monin, L. et al. Safety and immunogenicity of one versus two doses of the COVID-19 vaccine BNT162b2 for patients with cancer: interim analysis of a prospective observational study. *Lancet Oncol.* **22**, 765–778 (2021).
- Voysey, M. et al. Safety and efficacy of the ChAdOx1 nCoV-19 vaccine (AZD1222) against SARS-CoV-2: an interim analysis of four randomised controlled trials in Brazil, South Africa, and the UK. *Lancet* **397**, 99–111 (2021).
- Galván-Román, J. M. et al. IL-6 serum levels predict severity and response to tocilizumab in COVID-19: an observational study. *J. Allergy Clin. Immunol.* **147**, 72–80.e78 (2021).
- Hay, K. A. et al. Kinetics and biomarkers of severe cytokine release syndrome after CD19 chimeric antigen receptor–modified T-cell therapy. *Blood* **130**, 2295–2306 (2017).
- Chen, L. Y. C., Hoiland, R. L., Stukas, S., Wellington, C. L. & Sekhon, M. S. Assessing the importance of interleukin-6 in COVID-19. *Lancet Resp. Med.* **9**, e13 (2021).
- Morgan, C. J. Landmark analysis: a primer. *J. Nucl. Cardiol.* **26**, 391–393 (2019).
- Sahin, U. et al. An RNA vaccine drives immunity in checkpoint-inhibitor-treated melanoma. *Nature* **585**, 107–112 (2020).
- Sahin, U. et al. COVID-19 vaccine BNT162b1 elicits human antibody and T_H1 T cell responses. *Nature* **586**, 594–599 (2020).
- Liang, F. et al. Efficient targeting and activation of antigen-presenting cells in vivo after modified mRNA vaccine administration in rhesus macaques. *Mol. Ther.* **25**, 2635–2647 (2017).
- Pelka, K. et al. Spatially organized multicellular immune hubs in human colorectal cancer. *Cell* <https://doi.org/10.1016/j.cell.2021.08.003> (2021).
- Maslov, D. V. et al. Timing of steroid initiation and response rates to immune checkpoint inhibitors in metastatic cancer. *J. Immunother. Cancer* **9**, e002261 (2021).
- Iorgulescu, J. B. et al. Concurrent dexamethasone limits the clinical benefit of immune checkpoint blockade in glioblastoma. *Clin. Cancer Res.* **27**, 276–287 (2021).
- Valachis, A. et al. Improved survival without increased toxicity with influenza vaccination in cancer patients treated with checkpoint inhibitors. *Oncot Immunology* **10**, 1886725 (2021).
- Sun, Z. et al. A next-generation tumor-targeting IL-2 preferentially promotes tumor-infiltrating CD8⁺ T-cell response and effective tumor control. *Nat. Commun.* **10**, 3874 (2019).
- Mevorach, D. et al. Myocarditis after BNT162b2 mRNA vaccine against Covid-19 in Israel. *N. Engl. J. Med.* **385**, 2140–2149 (2021).
- Phillips, R., Hazell, L., Sauzet, O. & Cornelius, V. Analysis and reporting of adverse events in randomised controlled trials: a review. *BMJ Open* **9**, e024537 (2019).
- Strobel, S.B., Machiraju, D., Kälber, K.A. & Hassel, J.C. Immune-related adverse events of COVID-19 vaccination in skin cancer patients receiving immune-checkpoint inhibitor treatment. *Cancer Immunol. Immunother.* <https://doi.org/10.1007/s00262-021-03133-w> (2021).
- Moore, H. M. et al. Biospecimen reporting for improved study quality (BRISQ). *Cancer Cytopathol.* **119**, 92–102 (2011).
- Miroglio, B., Zeber, D., Kaye, J. & Weiss, R. The effect of ad blocking on user engagement with the web. In: *Proc. 2018 World Wide Web Conference* 813–821 (International World Wide Web Conferences Steering Committee, Lyon, France, 2018).
- Walle, T. Wallet-maker/ANTICIPATE_COVID-19. *Zenodo* <https://zenodo.org/record/6544522#.YoYUQXXMLcs> (2022).

Acknowledgements

We thank all participating patients and their relatives for their consent to this research. Kind help in recruiting patients was provided by NCT Day Clinic 1, Day Clinic 2 and Dermatology Outpatient Clinic nursing staff whom we thank for blood sampling. We express gratitude to the DKFZ Flow Cytometry Core Facility for technical support and infrastructure. Biomaterial samples were provided by the Liquid Biobank of the NCT Heidelberg, in accordance with the regulations of the BioMaterialBank Heidelberg and the approval of the ethics committee of Heidelberg University. Interpretation of socioeconomic aspects of cancer therapy was kindly provided by E. Winkler and A. Züger. T.W. and A.S. have been funded by a fellowship of the DKFZ Clinician Scientist Program, supported by the Dieter Morszeck Foundation. Additional funding for blood sampling materials was provided by CanVirex to T.W. and G.U.

Author contributions

T.W. was responsible for conceptualization. T.W., J.A.K. and R.K. were responsible for the methodology. Computer code was developed by T.W. T.W., S.B., J.A.K., B.H., L.Z., R.S. and S.S. were responsible for the investigations. Patient recruitment was conducted by T.W., K.A.K., C.S.C., S.B.S., T.R., L.J.M., J.B., M.J., C.F., S.K., A.S., K.S., S.M.K., C.S.-T., C.S., J.B., T.D., E.B., M.C., X.Z., A.R., M.S., F.M., M.F.L., A.S., D.J., A.W., J.K., G.M.H., S.Z., L.A., A.K.B., N.H., R.K., J.C.H. and the NCT ANTICIPATE Investigators. T.W. wrote the original draft of the manuscript. T.W., S.B., G.U., J.A.K., G.M.H., A.K.B. and C.S. reviewed and edited the manuscript. T.W. and S.B. were responsible for visualization. T.W. and G.U. were responsible for funding acquisition. G.U. supervised the study. J.K. and R.Z.K. provided statistical consultation.

Funding

Open access funding provided by Deutsches Krebsforschungszentrum (DKFZ).

Competing interests

T.W. reports previous and current stock ownership of various pharmaceutical companies manufacturing SARS-CoV-2 vaccines and diagnostics including BionTech, Astra Zeneca and Roche. T.W. also reports research support from CanVirex, a spin-off company of the Heidelberg University Hospital developing viral vector-based immunotherapies and vaccines (financial support for blood sampling materials). G.U. is founder and current CMO/CSO of CanVirex, Basel, Switzerland. G.M.H. reports consulting or advisory roles (unrelated) at Bristol-Myers Squibb, MSD Sharp & Dohme, Lilly, Novartis and Daiichi Sankyo; honoraria (unrelated) from Servier, MSD Sharp & Dohme, Lilly, Targos, Bristol-Myers Squibb, IOMEDICO and MCI Conventions; research funding (unrelated) from Nordic Pharma, Taiho Pharmaceutical, MSD Sharp & Dohme, Janssen, Astra Zeneca and IKF Klinische Krebsforschung Frankfurt; and travel/accommodations (unrelated) from Bristol-Myers Squibb, Lilly, Servier and MSD Sharp & Dohme. All other authors declare no competing interests.

Additional information

Extended data is available for this paper at <https://doi.org/10.1038/s43018-022-00398-7>.

Supplementary information The online version contains supplementary material available at <https://doi.org/10.1038/s43018-022-00398-7>.

Correspondence and requests for materials should be addressed to Thomas Walle.

Peer review information *Nature Cancer* thanks Nicole Kuderer, Song Liu and Jason Goldman for their contribution to the peer review of this work.

Reprints and permissions information is available at www.nature.com/reprints.

Publisher's note Springer Nature remains neutral with regard to jurisdictional claims in published maps and institutional affiliations.



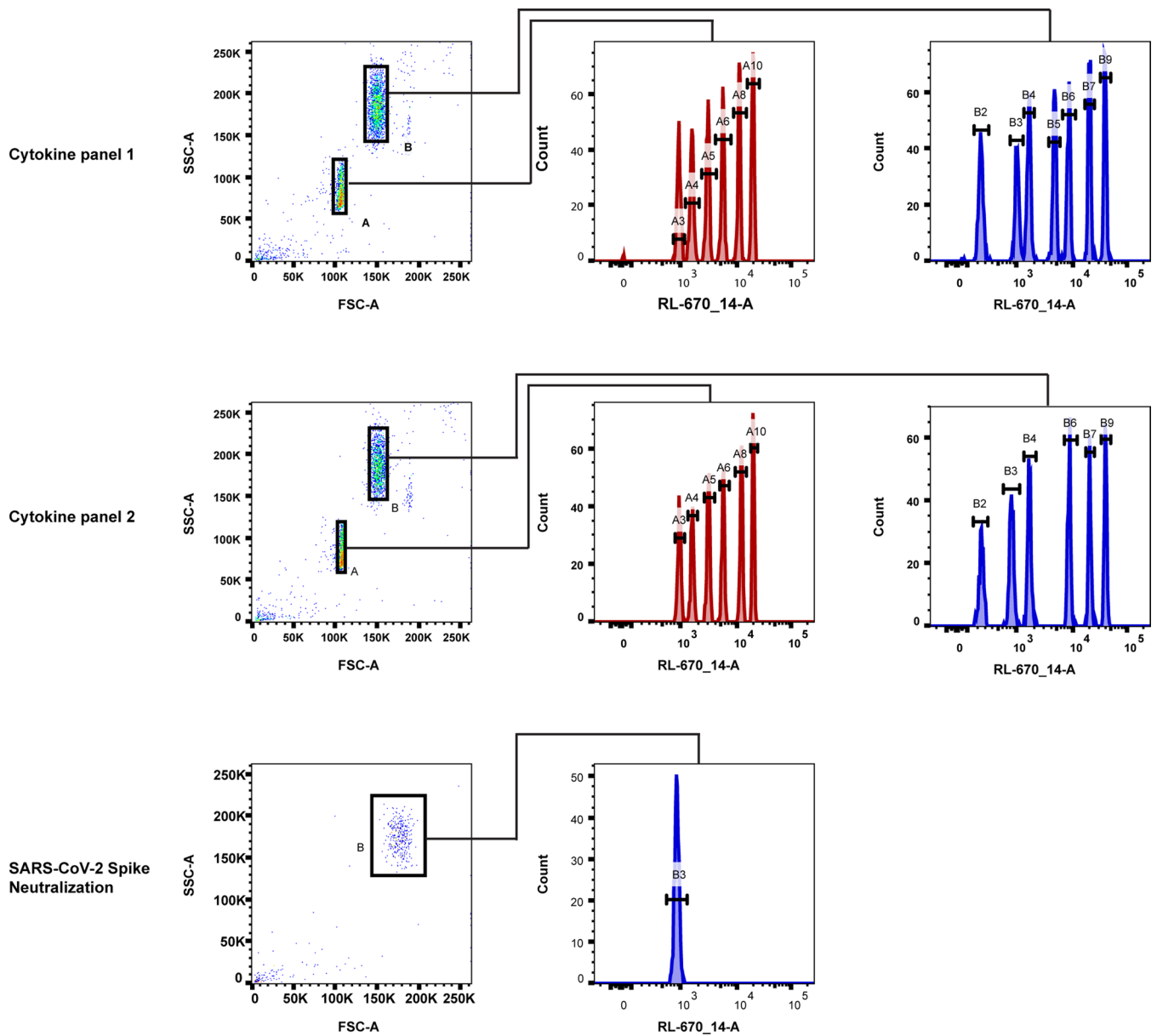
Open Access This article is licensed under a Creative Commons Attribution 4.0 International License, which permits use, sharing, adaptation, distribution and reproduction in any medium or format, as long as you give appropriate credit to the original author(s) and the source, provide a link to the Creative Commons license, and indicate if changes were made. The images or other third party material in this article are included in the article's Creative Commons license, unless indicated otherwise in a credit line to the material. If material is not included in the article's Creative Commons license and your intended use is not permitted by statutory regulation or exceeds the permitted use, you will need to obtain permission directly from the copyright holder. To view a copy of this license, visit <http://creativecommons.org/licenses/by/4.0/>.

© The Author(s) 2022, corrected publication 2022

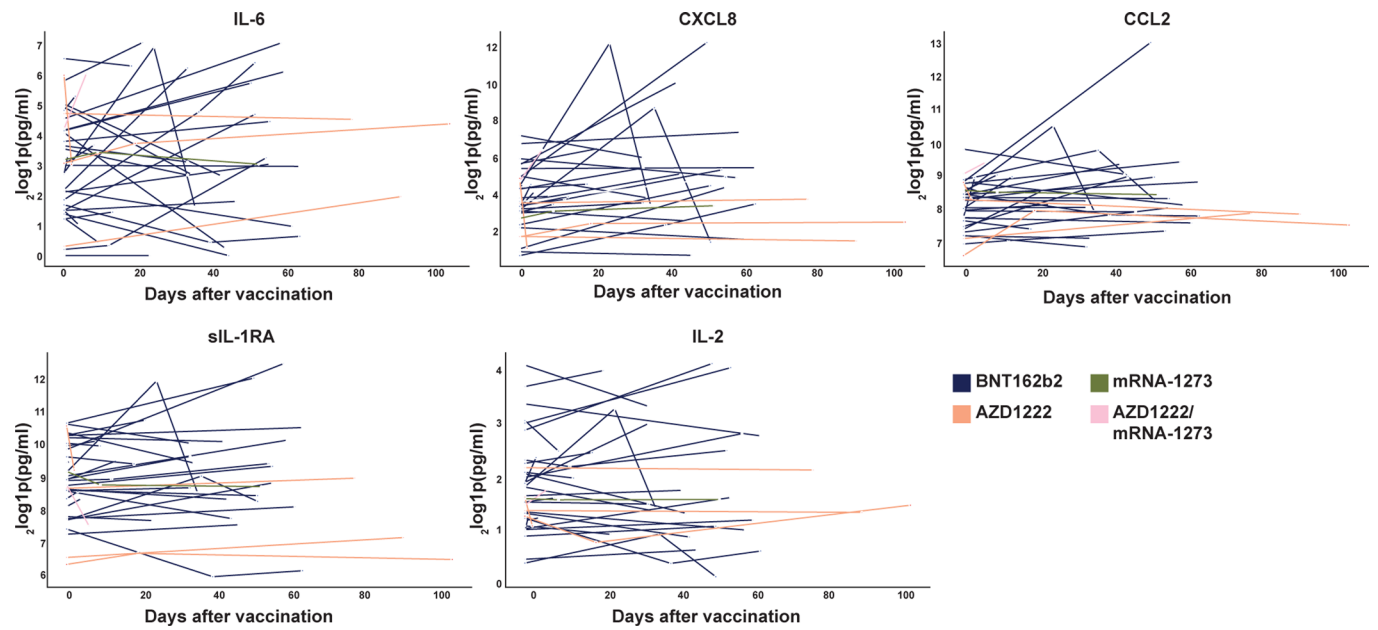
NCT ANTICIPATE Investigators

Thomas Walle^{1,2,3,19}, Joscha A. Kraske², Thomas Rösner², Christiane S. Cussigh⁴, Katharina A. Kälber⁴, Lisa Jasmin Müller⁵, Sophia Boyoung Strobel⁴, Jana Burghaus⁴, Stefan M. Kallenberger², Christoph K. Stein-Thöringer^{2,6}, Maximilian Jenzer², Antonia Schubert^{2,3,7,8}, Steffen Kahle², Anja Williams², Omar Abdelrahim², Elena Busch², Patrick Derigs⁵, Katharina Dischinger², Fouad Mitri⁴, Kerstin Schmidt², Irfan A. Bhatti², Barbara Grün², Nicolas Hohmann², Lena Woydack², Xin-Wen Zhang², Dyke Ferber², Andreas Mock², Tillmann Pompecki¹⁸, Timo Schank⁴, Carlo Fremd^{3,12}, Andreas Schneeweiss¹², Jürgen Krauss², Leonidas Apostolidis², Anne Katrin Berger², Georg M. Haag^{2,12}, Stefanie Zschäbitz², Niels Halama^{2,13,14,15}, Christoph Springfield², Romy Kirsten¹⁸, Jessica C. Hassel⁵, Dirk Jäger^{2,12} and Guy Ungerechts^{1,2,16,17}

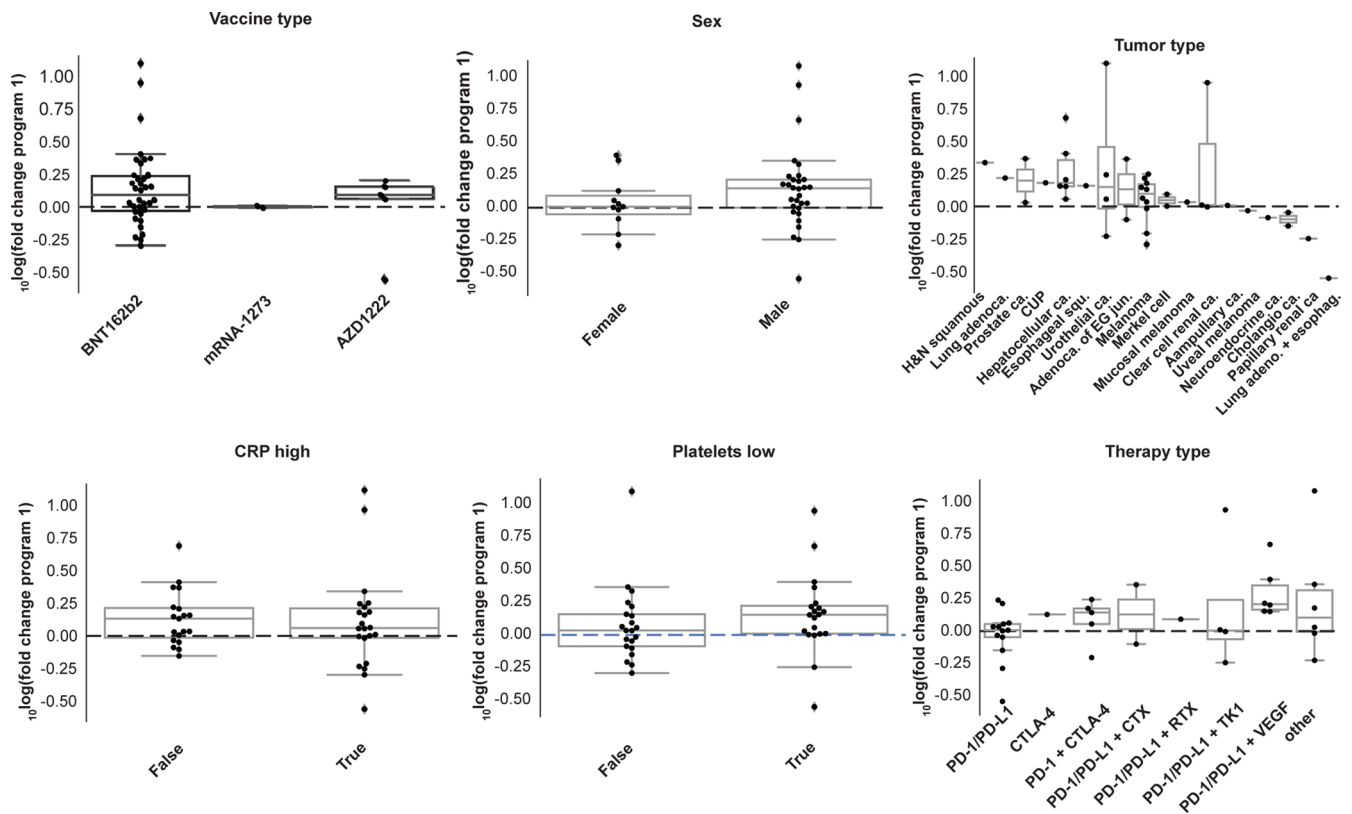
¹⁸Department of Gastroenterology, Heidelberg University Hospital, Heidelberg, Germany.



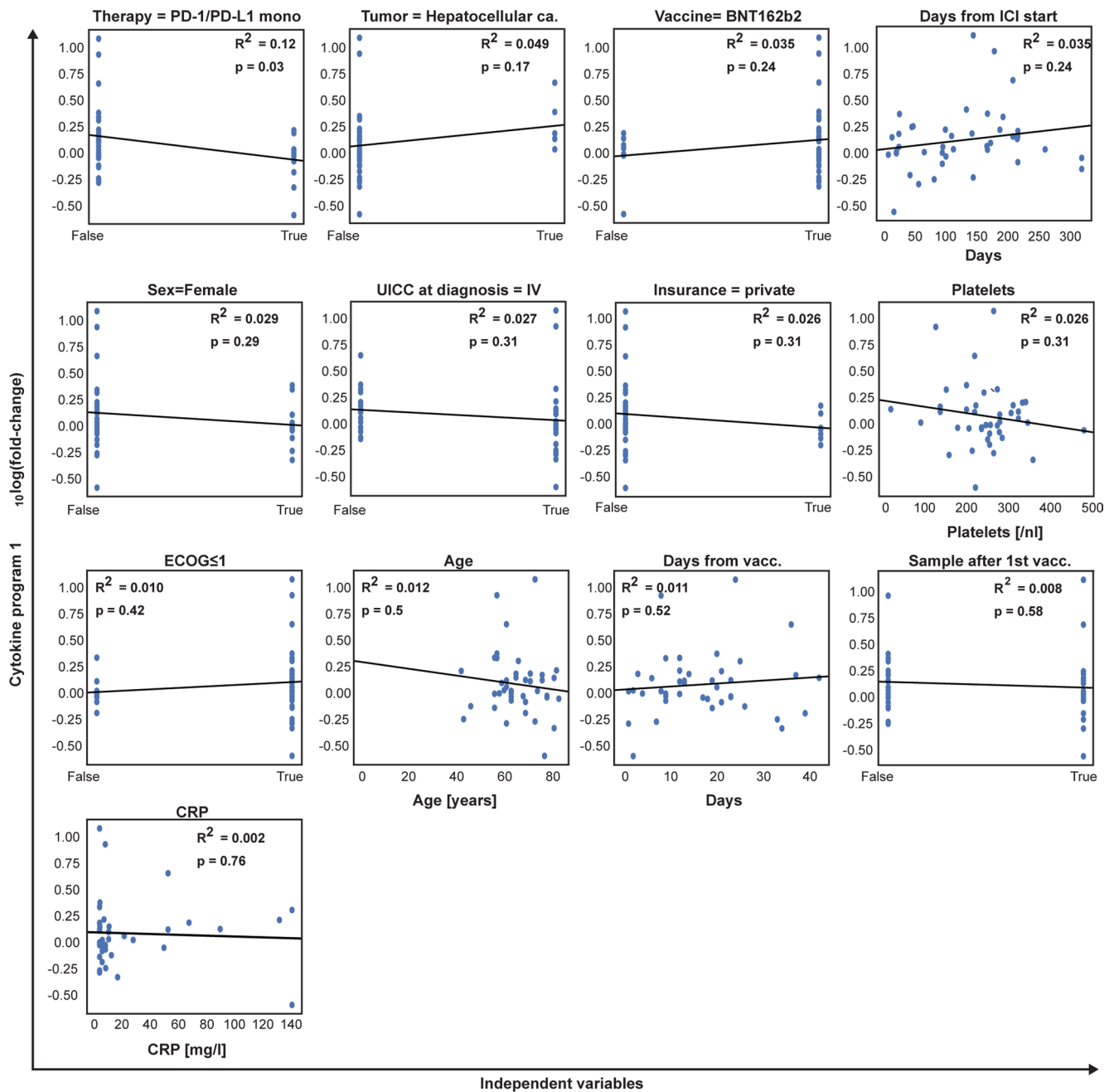
Extended Data Fig. 1 | Gating strategy for flow-cytometry based multiplex cytokine array, related to Fig. 3. Schema outlining the gating strategy used in the multiplex cytokine arrays and neutralizing antibody assay to define bead populations based on sideward-scatter (SSC), forward-scatter (FSC) and fluorescence signal in the red laser 670/14 channel. First row indicating gating schemas for cytokine panel 1 (741091, Biolegend, CA, USA), second row indicating gating for cytokine panel 2 (741142, Biolegend, CA, USA) and third row indicating gating for SARS-CoV-2 Neutralizing Antibody Assay (741127, Biolegend, CA, USA).



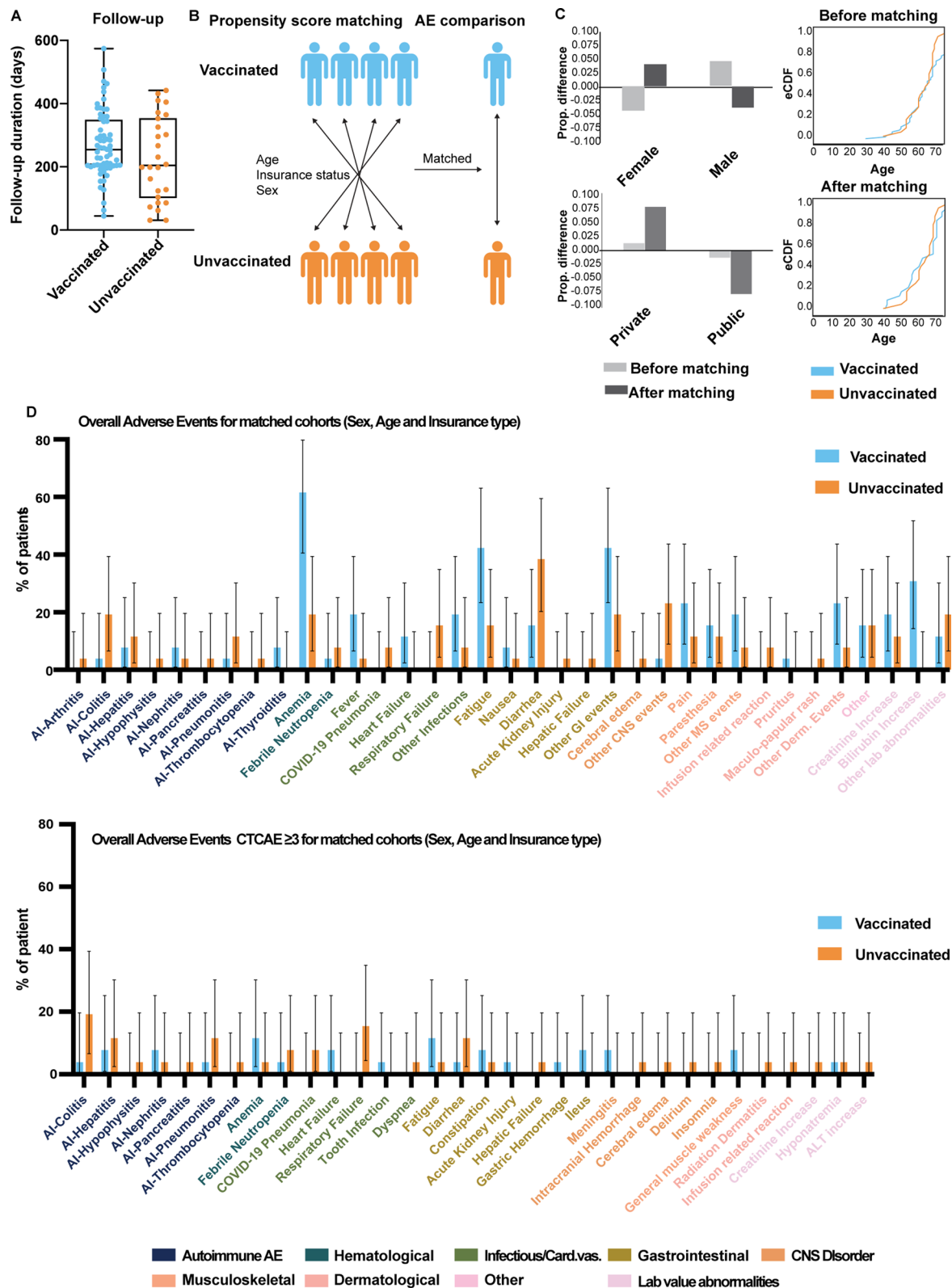
Extended Data Fig. 2 | Cytokine concentrations in COVID-19 vaccinated patients, related to Fig. 3. Line-plots indicating log_{1p} transformed individual cytokine concentrations of cytokine program 1 cytokines after vaccination in $n = 35$ patients. $\log_{1p}(x) = {}_{10}\log(x + 1)$ with x : cytokine concentration in pg/ml.



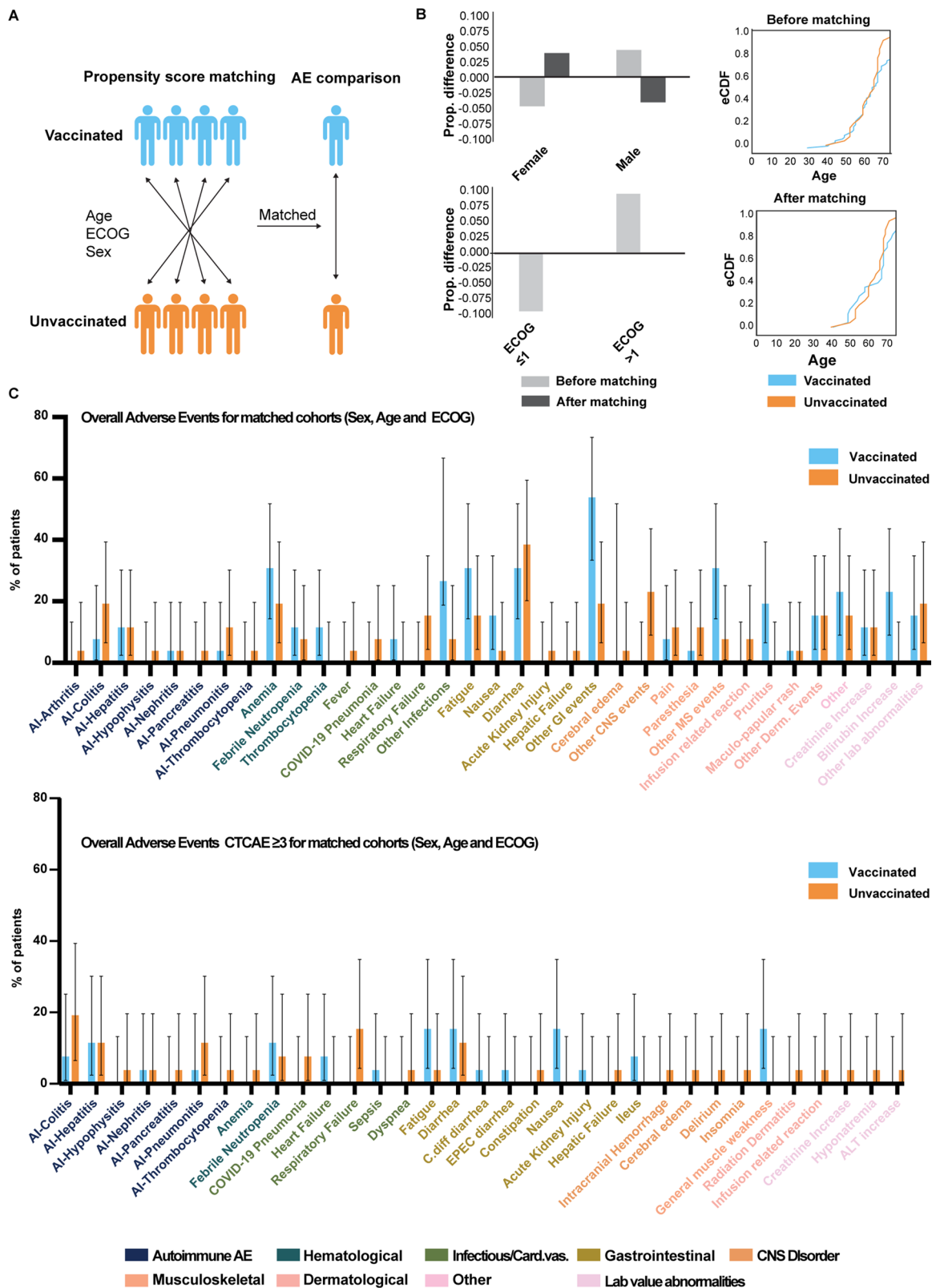
Extended Data Fig. 3 | Cytokine program 1 upregulation stratified by patient characteristics, related to Fig. 3. Box-plots indicating median $_{10}\log(\text{fold change})$ of cytokine program 1 after COVID-19 vaccination (horizontal lines) with inter-quartile range (boxes) and range (whiskers, range calculation not including outliers as implemented in `seaborn.boxplot` function) stratified according to vaccine type (left upper panel), sex (middle upper panel), tumor type (right upper panel), above or below median of maximum CRP after vaccination (after 1st vaccination dose for cytokine samples after 1st vaccination or after 2nd vaccination dose for cytokine samples after 2nd vaccination), above or below median of minimum platelet counts after vaccination (after 1st vaccination dose for cytokine samples after 1st vaccination or after 2nd vaccination dose for cytokine samples after 2nd vaccination) or by therapy type ($n = 41$ patient samples).



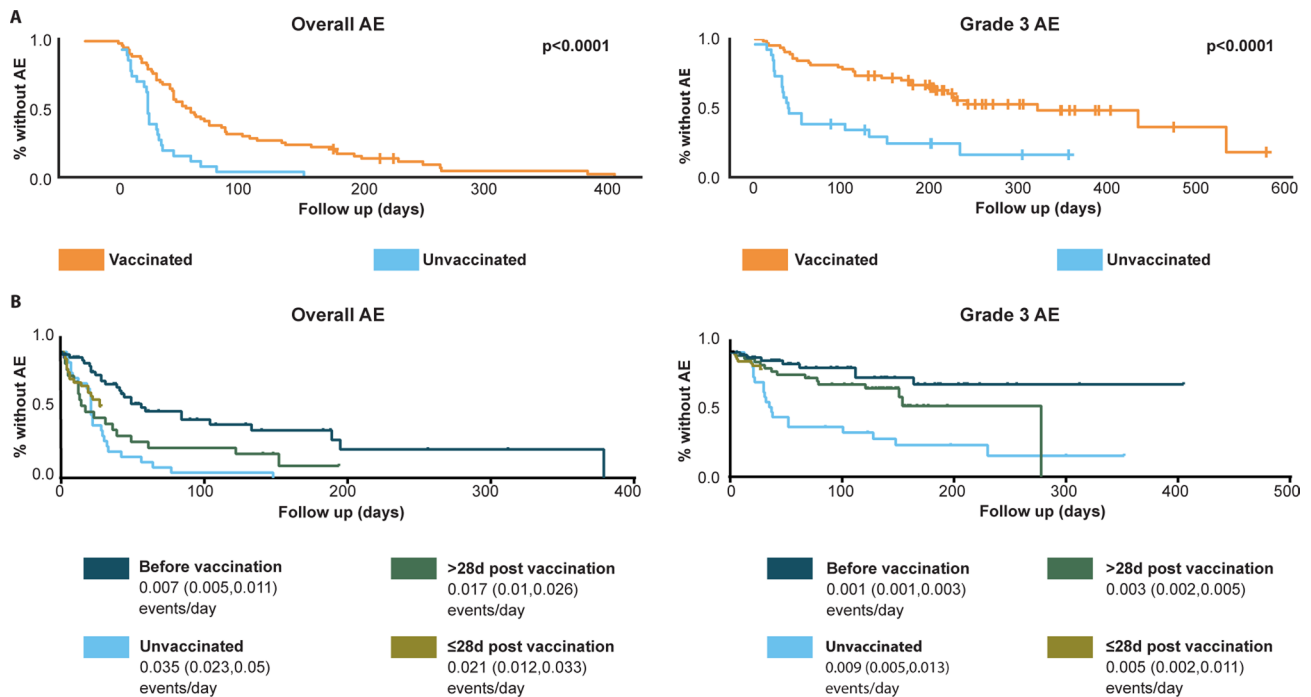
Extended Data Fig. 4 | Univariate linear regression for cytokine program 1, related to Fig. 3. Scatter plots indicating average $_{10}\log(\text{fold change})$ of cytokine program 1 after COVID-19 vaccination (dependent variable) in relation to different clinical variables (independent variables). Boolean variables True and False on the x axis refer to the variable indicated in the header. Lines indicate the regressed function with p values (two-sided) not corrected for multiple comparisons and R^2 values indicated in each panel (n = 41 patient samples).



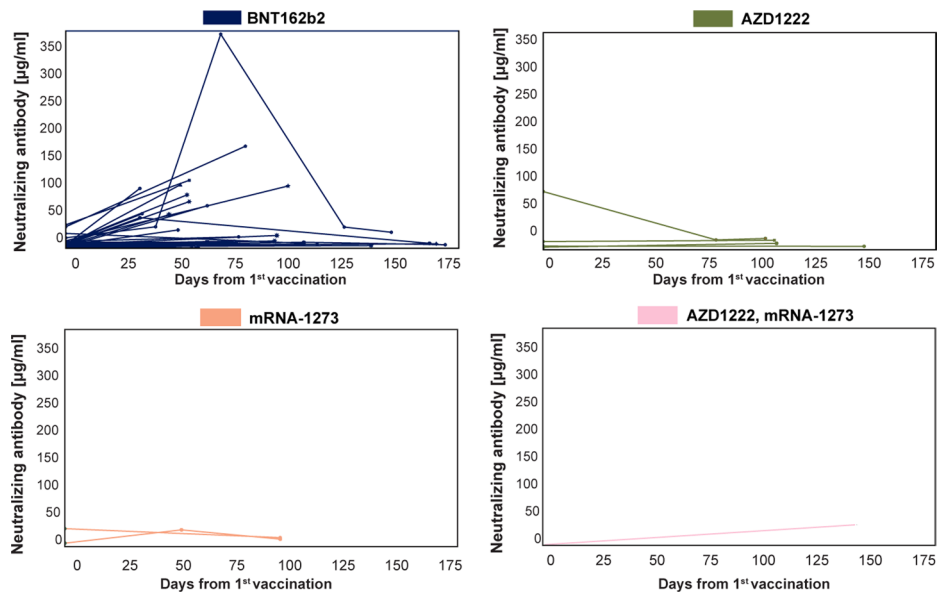
Extended Data Fig. 5 | Adverse events in sex, age, insurance type matched COVID-19-vaccinated and unvaccinated immune checkpoint therapy treated patients with cancer, related to Fig. 4. (a) Box and whiskers plot depicting the total follow-up duration (days) for vaccinated ($n=64$) and unvaccinated ($n=26$) patients. The whiskers indicate range, the box the upper and lower quartile and the horizontal bar the median. (b) Schema indicating the propensity score based matching procedure. (c) Bar graphs indicating the proportional difference of sex and insurance status before and after propensity score matching (upper panel, $n=26$ unvaccinated and $n=26$ matched vaccinated patients). Xy plot indicating the empirical cumulative distribution function (eCDF) of vaccinated ($n=26$) and unvaccinated ($n=26$) patients before and after matching. (d) Bar graphs indicating frequencies and error bars the 95% confidence interval of all (upper panel) or grade ≥ 3 (lower panel) adverse events in matched vaccinated ($n=26$) and unvaccinated ($n=26$) patients. This is proportional data therefore the confidence interval is asymmetric and the center is the bar.



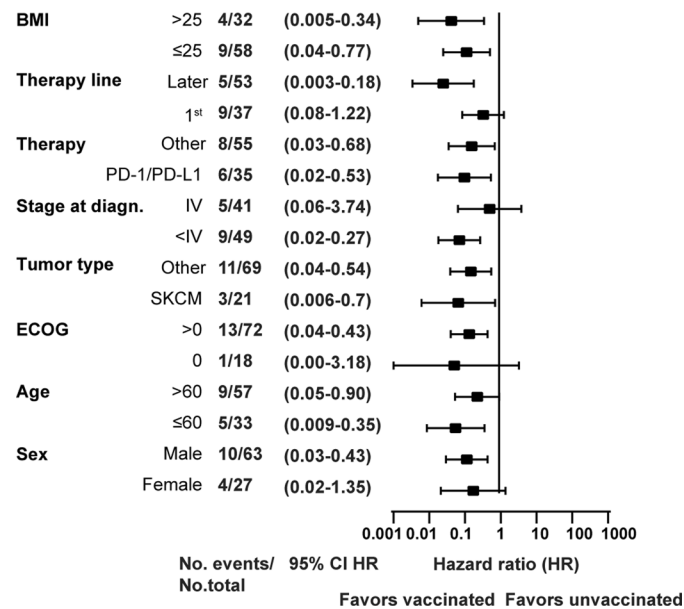
Extended Data Fig. 6 | Adverse events in sex, age, ECOG matched COVID-19-vaccinated and unvaccinated immune checkpoint therapy treated cancer patients, related to Fig. 4. (a) Schema indicating the propensity score based matching procedure. (b) Bar graphs indicating the proportional difference of sex and ECOG before and after propensity score matching (upper panel, $n = 26$ unvaccinated and $n = 26$ matched vaccinated patients). Xy plot indicating the empirical cumulative distribution function (eCDF) of vaccinated ($n = 26$) and unvaccinated ($n = 26$) patients before and after matching. (c) Bar graphs indicating frequencies and error bars the 95% confidence interval of all (upper panel) or grade ≥ 3 (lower panel) adverse events in matched vaccinated ($n = 26$) and unvaccinated ($n = 26$) patients. This is proportional data therefore the confidence interval is asymmetric and the center is the bar.



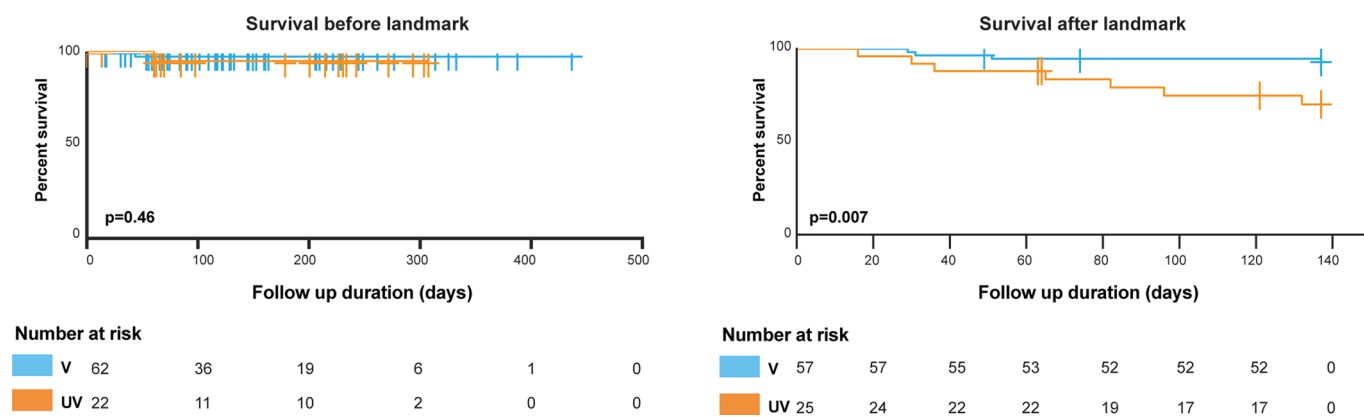
Extended Data Fig. 7 | Time to adverse event analysis, related to Fig. 4. (a) Kaplan-Meier curves indicating the time without any (left panel) or \geq CTCAE ≥ 3 adverse event (right panel) for vaccinated ($n = 64$) and unvaccinated patients ($n = 26$) over the entire course of immune checkpoint therapy with the legend indicated below. P values (two-sided) were calculated using logrank tests (any AE: test statistic = 19.4, grade ≥ 3 AE: test statistic = 18.7). Exact p values: $1.0475761018388364 \times 10^{-5}$ (left panel), $1.5047888131226484 \times 10^{-5}$ (right panel). (b) Kaplan-Meier curves indicating the time without any (left panel) or \geq CTCAE ≥ 3 adverse event (right panel) for unvaccinated patients ($n = 26$) over the entire course of immune checkpoint therapy and for vaccinated patients before ($n = 48$) vaccination, up to 28 days ($n = 21$) after vaccination and longer than 28 days ($n = 37$) after vaccination. The color code, average events per day and their 95% confidence intervals (in parenthesis) are indicated in the legend below.



Extended Data Fig. 8 | S1 neutralizing antibody concentrations after COVID-19 vaccination in ICI-treated patients, related to Fig. 4. Line-plots indicating neutralizing antibody concentrations of n=40 individual patients after vaccination as assessed by an ACE2 S1 competitive immunoassay (research grade). Color code indicating vaccine type in the respective patients.



Extended Data Fig. 9 | Vaccination is associated with prolonged overall survival probability across patient subgroups, related to Fig. 4. Forest-plot indicating hazard ratios (HR, squares) and 95% confidence intervals (CI, whiskers) of vaccinated (n=26) and unvaccinated (n=64) patients stratified into the subgroups indicated with the exact number (no.) of events and patients at risk for each subgroup as well as the 95% CIs indicated on the left. Hazard ratios and confidence intervals were calculated using a Log-rank test or if no events were observed in one group with the Mantel-Hanszel method. sex - female: test statistic = 3.2, sex - male: test statistic = 11.3, age ≤60: test statistic = 9.4, age >60: test statistic = 4.4, ECOG 0: test statistic = 2.0, ECOG >0: test statistic = 10.6, tumor type = melanoma: test statistic = 5.1, tumor type = other: test statistic = 11.1, stage <4: test statistic = 14.9, stage 4: test statistic = 0.7, therapy = PD-1/PD-L1 mono: test statistic = 7.1, therapy = other: test statistic = 7.0, therapy line = 1st: test statistic = 3.1, therapy line = other: test statistic = 13.5, BMI >25: test statistic = 8.8, BMI ≤25: test statistic = 8.2. Diagn.: diagnosis.



Extended Data Fig. 10 | Landmark survival analysis in COVID-19 vaccinated and unvaccinated patients, related to Fig. 4. Kaplan-Meier curves indicating overall survival of COVID-19 vaccinated and unvaccinated immune checkpoint inhibitor treated cancer patients. Survival was analyzed before (left panel) or after (right panel) said landmark. Only patients who gave informed consent until the landmark were included in this analysis. The landmark was defined as 17th May 2020, the date of general eligibility for COVID-19 vaccination for the entire adult population in the state of Baden-Württemberg, Germany. P values (two-sided) were calculated using logrank tests (before landmark: test statistic = 0.5 n = 22 unvaccinated, n = 62 vaccinated, after landmark: test statistic = 7.1 n = 25 unvaccinated, n = 57 vaccinated).

Reporting Summary

Nature Portfolio wishes to improve the reproducibility of the work that we publish. This form provides structure for consistency and transparency in reporting. For further information on Nature Portfolio policies, see our [Editorial Policies](#) and the [Editorial Policy Checklist](#).

Statistics

For all statistical analyses, confirm that the following items are present in the figure legend, table legend, main text, or Methods section.

n/a Confirmed

- The exact sample size (n) for each experimental group/condition, given as a discrete number and unit of measurement
- A statement on whether measurements were taken from distinct samples or whether the same sample was measured repeatedly
- The statistical test(s) used AND whether they are one- or two-sided
Only common tests should be described solely by name; describe more complex techniques in the Methods section.
- A description of all covariates tested
- A description of any assumptions or corrections, such as tests of normality and adjustment for multiple comparisons
- A full description of the statistical parameters including central tendency (e.g. means) or other basic estimates (e.g. regression coefficient) AND variation (e.g. standard deviation) or associated estimates of uncertainty (e.g. confidence intervals)
- For null hypothesis testing, the test statistic (e.g. F , t , r) with confidence intervals, effect sizes, degrees of freedom and P value noted
Give P values as exact values whenever suitable.
- For Bayesian analysis, information on the choice of priors and Markov chain Monte Carlo settings
- For hierarchical and complex designs, identification of the appropriate level for tests and full reporting of outcomes
- Estimates of effect sizes (e.g. Cohen's d , Pearson's r), indicating how they were calculated

Our web collection on [statistics for biologists](#) contains articles on many of the points above.

Software and code

Policy information about [availability of computer code](#)

Data collection Data was collected from patient electronic health records or FCS files generated using BD FACS DIVA v8.0.

Data analysis All custom code is provided under an MIT license <https://doi.org/10.5281/zenodo.6544522>
Data was analyzed in python 3 using Jupyter Notebook (v1.0.0) and included the following open source software packages:

```
imgaug==0.2.5
matplotlib==3.4.3
pandas==0.23.4
squarify==0.4.3
lifelines==0.26.4
statsmodels==0.10.2
numpy==1.19.5
seaborn==0.11.2
mpmath==1.2.1
scipy==1.4.1
pymatch==0.3.4
jupyter==1.0.0
```

Flow cytometry data was analyzed using Legendplex Software v 2021.07.01 (Biolegend, San Diego, CA, U.S.A.).
Statistical analysis and plotting was performed with GraphPad Prism 9.2.0 (GraphPad Software, San Diego, CA, U.S.A.).
Multiple comparison p value correction was performed with R 4.1.1
Plots were arranged using Adobe Illustrator 2021 (25.2.2, Adobe Inc, San Jose, CA, USA).

All custom computer code used to generate the results in this study has been deposited in a GitHub repository (https://github.com/wallet-maker/ANTICIPATE_COVID-19.git) and a Zenodo repository (<https://doi.org/10.5281/zenodo.6544522>) under an MIT license.

For manuscripts utilizing custom algorithms or software that are central to the research but not yet described in published literature, software must be made available to editors and reviewers. We strongly encourage code deposition in a community repository (e.g. GitHub). See the Nature Portfolio [guidelines for submitting code & software](#) for further information.

Data

Policy information about [availability of data](#)

All manuscripts must include a [data availability statement](#). This statement should provide the following information, where applicable:

- Accession codes, unique identifiers, or web links for publicly available datasets
- A description of any restrictions on data availability
- For clinical datasets or third party data, please ensure that the statement adheres to our [policy](#)

The patient data that support the findings of this study are available in pseudonymized form open access in zenodo with the identifiers: 10.5281/zenodo.6544522. This includes clinical metadata including survival as well as primary data on cytokine concentrations and neutralizing antibody concentrations. Data is available until 8th December 2031 for 10 years as consented to by the study participants. The trial has been prospectively registered and the study protocol including the statistical analysis plan is available under the German Clinical Trial Register (<https://drks.de>) under the accession number DRKS00022890. No custom materials have been generated during this study.

Field-specific reporting

Please select the one below that is the best fit for your research. If you are not sure, read the appropriate sections before making your selection.

- Life sciences Behavioural & social sciences Ecological, evolutionary & environmental sciences

For a reference copy of the document with all sections, see [nature.com/documents/nr-reporting-summary-flat.pdf](https://www.nature.com/documents/nr-reporting-summary-flat.pdf)

Life sciences study design

All studies must disclose on these points even when the disclosure is negative.

| | |
|-----------------|--|
| Sample size | Sample size estimation was performed for the primary outcome of this study prediction of radiological response which will be reported elsewhere. Based on a meta-analysis of current clinically applied predictors to PD-1/PD-L1 immune checkpoint blockade (10.1001/jamaoncol.2019.1549), we defined an AUC of >0.78 as a clinically relevant threshold above the current biomarker predictive power. To assess the potential predictive power of using the immune cell composition as a biomarker we used published data from renal cell carcinoma patients undergoing combined nivolumab and ipilimumab immune checkpoint therapy to calculate a receiver operator curve (10.1038/s41591-019-0694-x). Based on this AUC confidence intervals for different numbers of patients were calculated assuming a response rate of 10% to immune checkpoint therapy. This response rate is the average response rate in poorly responding tumor types, which likely represent the majority of our patients at our center. In our sample size estimation, a patient number of n=200 resulted in a lower 95% confidence interval of AUC=0.782, which was above our predefined clinically relevant threshold. We estimate a drop-out of 10% due to loss to follow-up of the patients resulting in a total of 220 patients for the training/exploration cohort reported here. |
| Data exclusions | We excluded one patient who had an immune related adverse event (arthritis grade 3) at baseline before vaccination because this not vaccine related event could have confounded immunological analyses |
| Replication | Cytokine concentrations and neutralizing antibody concentrations were measured in duplicates. Cytokine concentrations were measured in 3 independent experiments on different patients all with similar results (replication successful). Antibody concentrations were assessed in one experiments. |
| Randomization | This is a cohort study, no randomization was performed. We used a multivariate Cox proportional hazards model to assess the effects of different covariates (ECOG, line of therapy, age, mono vs combination immunotherapy, sex, tumor type, tumor stage, insurance status, vaccination status) on survival outcomes. For adjusting covariates for adverse event analysis we performed propensity score matching with the propensity score calculated either on sex, age and ECOG or on sex, age and insurance status. |
| Blinding | For cytokine concentration data the acquisition and processing of the raw data was performed by a clinician scientist who was blinded to the patients' identity and metadata and who was not involved in downstream data analysis. Notably, the patients' pseudonyms contained the temporal sequence of the samples. |

Reporting for specific materials, systems and methods

We require information from authors about some types of materials, experimental systems and methods used in many studies. Here, indicate whether each material, system or method listed is relevant to your study. If you are not sure if a list item applies to your research, read the appropriate section before selecting a response.

Materials & experimental systems

Methods

| n/a | Involved in the study |
|-------------------------------------|---|
| <input type="checkbox"/> | <input checked="" type="checkbox"/> Antibodies |
| <input checked="" type="checkbox"/> | <input type="checkbox"/> Eukaryotic cell lines |
| <input checked="" type="checkbox"/> | <input type="checkbox"/> Palaeontology and archaeology |
| <input checked="" type="checkbox"/> | <input type="checkbox"/> Animals and other organisms |
| <input type="checkbox"/> | <input checked="" type="checkbox"/> Human research participants |
| <input type="checkbox"/> | <input checked="" type="checkbox"/> Clinical data |
| <input checked="" type="checkbox"/> | <input type="checkbox"/> Dual use research of concern |

| n/a | Involved in the study |
|-------------------------------------|--|
| <input checked="" type="checkbox"/> | <input type="checkbox"/> ChIP-seq |
| <input type="checkbox"/> | <input checked="" type="checkbox"/> Flow cytometry |
| <input checked="" type="checkbox"/> | <input type="checkbox"/> MRI-based neuroimaging |

Antibodies

| | |
|-----------------|---|
| Antibodies used | Legendplex Cytokine Storm Panel 1 (AB_2895549 (antibodyregistry.org), 741091, Biolegend, CA, USA), Cytokine Storm Panel 2 (AB_2895550 (antibodyregistry.org), 741142, Biolegend, CA, USA), SARS-CoV-2 Neutralizing Antibody Assay (AB_2895551 (antibodyregistry.org), 741127, Biolegend, CA, USA) |
| Validation | The antibodies of the Cytokine Storm Panels have been validated for sensitivity, accuracy and cross-reactivity with 27 different cytokines, linearity of dilution and inter-/intra-assay precision. Minimal cross-reactivity was observed. Accuracy (spike recovery) was between 33% (IL-13) and 162% (APRIL) in human serum. The neutralizing antibody assay was also validated for sensitivity, cross-reactivity against non-neutralizing antibody and accuracy (spike recovery 90% in serum) as well as linearity of dilution, inter- and intra-assay precision. |

Human research participants

Policy information about [studies involving human research participants](#)

| | |
|----------------------------|--|
| Population characteristics | Adult patients with advanced solid tumors starting a new cancer immunotherapy either as mono- or combination therapy except adoptive cell therapies were included in this study. Patients were included regardless of sex. Detailed characteristics can be found in Table 1 of the manuscript. |
| Recruitment | Patients were identified by screening for patients with solid tumors that were to receive combinatorial immune checkpoint therapies (ICT). These patients were informed of the possibility of inclusion in our study before induction of ICT and their informed consent was obtained. Self-selection bias could have presented patients with severe disease from participating. As per German law study inclusion/exclusion criteria prohibited inclusion of non-German speakers because they would be considered unable to understand all details of the informed consent resulting in a possible bias towards excluding immigrants. Patient recruitment is outlined in the CONSORT flow chart in Figure 1A |
| Ethics oversight | The trial received institutional ethics review board approval at Ethics Commission I Medical Faculty Heidelberg, Heidelberg University (S-373/2020, S-207/2005,) and Ethics Commission II Medical Faculty Mannheim, Heidelberg University (2021-567). |

Note that full information on the approval of the study protocol must also be provided in the manuscript.

Clinical data

Policy information about [clinical studies](#)

All manuscripts should comply with the ICMJE [guidelines for publication of clinical research](#) and a completed [CONSORT checklist](#) must be included with all submissions.

| | |
|-----------------------------|--|
| Clinical trial registration | German Clinical Trial Registry (DRKS): DRKS00022890 |
| Study protocol | Study protocol available under the registry number at www.drks.de . |
| Data collection | Recruitment for this exploration cohort of the prospective study was performed between 12/2019 and 07/2021. Data and patient sample collection began at the date of first patient recruitment (12/2019) until 1.10.2021 from electronic patient health records continuously updated by the treating physicians and trial staff at the National Center for Tumor Diseases, Heidelberg, Germany. |
| Outcomes | <p>The primary endpoint is radiological response to therapy for which a biomarker-based prediction model will be developed based on the immune cell composition and serum proteome and metabolome of these patients.</p> <p>Secondary endpoints include the immune cell and serum proteome and metabolome composition under IT and at disease progression, grade ≥ 3 adverse events including infections, as well as progression-free and overall survival. Select leukocyte subsets will be tested for cytotoxicity, migration, proliferation, metabolic function and cytokine production and differentiation properties in vitro and in xenograft mouse models. The effects of patient serum factors on these properties will also be investigated</p> |

Plots

Confirm that:

- The axis labels state the marker and fluorochrome used (e.g. CD4-FITC).
- The axis scales are clearly visible. Include numbers along axes only for bottom left plot of group (a 'group' is an analysis of identical markers).
- All plots are contour plots with outliers or pseudocolor plots.
- A numerical value for number of cells or percentage (with statistics) is provided.

Methodology

Sample preparation

Serum samples were thawed and immediately analyzed in duplicates using the Legendplex Cytokine Storm Panel 1 (741091, Biolegend, CA, USA), Cytokine Storm Panel 2 (741142, Biolegend, CA, USA) or SARS-CoV-2 Neutralizing Antibody Assay (741127, Biolegend, CA, USA) according to manufacturer's instructions (25ul detection antibody per sample) and analyzed on a BD FACS Canto II flow cytometer (BD, NJ, USA). Analyte concentrations were interpolated from a standard curve using 5 parameter logistic regression using Legendplex Software v 2021.07.01. Antibodies were validated by the manufacturer but not by our laboratory. The manufacturer does not disclose clone numbers for this assay.

Instrument

BD FACS Canto II

Software

BD FACS DIVA v8.0, Legendplex Software v 2021.07.01.

Cell population abundance

no cellular data was analyzed in this study

Gating strategy

Gating on detection beads was performed according to manufacturer instructions Legendplex Cytokine Storm Panel 1 (741091, Biolegend, CA, USA), Cytokine Storm Panel 2 (741142, Biolegend, CA, USA) or SARS-CoV-2 Neutralizing Antibody Assay (741127, Biolegend, CA, USA) .

- Tick this box to confirm that a figure exemplifying the gating strategy is provided in the Supplementary Information.